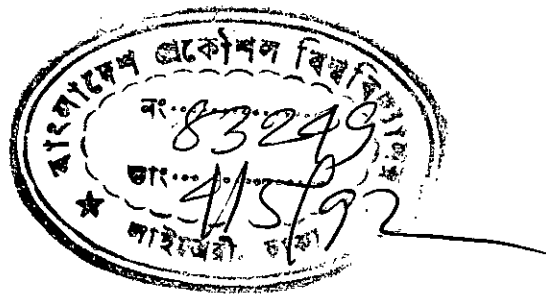


FLOW CHARACTERISTICS AROUND
RECTANGULAR CYLINDERS
IN TANDEM

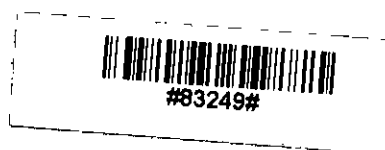
BY
MD. MOSHARROF HOSSAIN

A Thesis
Submitted to the Department of Mechanical Engineering in partial
fulfilment of the Requirements for the degree
of
MASTER OF SCIENCE IN MECHANICAL ENGINEERING



BANGLADESH UNIVERSITY OF ENGINEERING AND TECHNOLOGY, DHAKA

JUNE, 1991

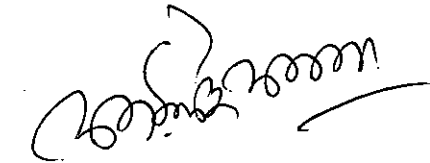


624.922
1991
MOS

RECOMMENDATION OF THE BOARD OF EXAMINERS

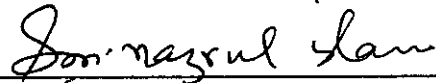
The Board of Examiners hereby recommends to the Department of Mechanical Engineering, Bangladesh University of Engineering and Technology, Dhaka, the acceptance of the thesis, " FLOW CHARACTERISTICS AROUND RECTANGULAR CYLINDERS IN TANDEM", submitted by Md. Mosharrof Hossain, in partial fulfilment of the requirements for the degree of Master of Science in Mechanical Engineering.

Chairman ;



Dr. A. K. M. Sadrul Islam
Associate Professor
Deptt. of Mechanical Engineering
BUET, Dhaka.

Member ;



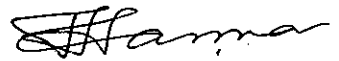
Dr. S. M. Nazrul Islam
Professor & Head
Deptt. of Mechanical Engineering
BUET, Dhaka.

Member ;



Dr. A. C. Mandal
Professor
Deptt. of Mechanical Engineering
BUET, Dhaka.

Member
(External) ;



Dr. Abdul Hannan
Professor
Deptt. of Water Resource Engg.
BUET, Dhaka.

June, 1991

ACKNOWLEDGEMENT

I express my deep sense of gratitude and profound indebtedness to Dr. A. K. M. Sadrul Islam for his guidance and supervision throughout the entire period of the experimental investigation. His initiatives, encouragement and invaluable suggestions are gratefully acknowledged without which this work would not have been possible.

I am highly grateful to Dr. M. a. Taher Ali, Dr. S. M. Nazrul Islam and Dr. A. C. Mandal for their constructive suggestions and co-operation.

I would like to thank Mr. A. M. Tito Islam for providing me with constructive suggestions and helping me solve many problems during the investigation. Without his kind co-operation and guidance this work could not have been carried out properly. I am also grateful to my friends and colleagues for their considerate attitude and profuse inspiration.

Sincere thanks are offered to Mr. Ahmed Ali Mollah, Chief Foreman Instructor, Machines Shop, BUET, Md. Rafiqul Islam, Foreman Instructor, Carpentry Shop, BUET, for their kind co-operation in the construction of the experimental set-up. Thanks are also due to Md. Shahabuddin, Faruque, Bachulal and Mozibar Rahman, technicians at the Fluid Mechanics Laboratory of Mechanical Engineering Department for their co-operation at different stages of the work. Thanks are due to Mr. Abdus Salam for Drafting the figures and Mr. Md. Abdul Jalil Sarder for typing the thesis.

Lastly, I would like to thank my wife who persistently kept me at my work and partly relieved me of family duties until this work was finished.

ABSTRACT

An experimental investigation of mean pressure distribution around two square cylinders in tandem is presented. Also the mean velocity distribution in the wake of the two cylinders were studied.

Pressure and velocity distributions were measured for various longitudinal spacings of the cylinders. Three different Reynolds numbers were taken into consideration. Drag and lift co-efficients were calculated by numerical integration.

A critical longitudinal spacing equal to four times the side dimension of the square cylinder ($L/D = 4$) was investigated. Beyond that critical spacing both the cylinders were subjected to drag force. When $L/D < 4$ only the downstream cylinder is subjected to negative drag (or thrust). Also the shape of the velocity profile behind upstream cylinder is different from that of single cylinder. However beyond $L/D = 4$ the nature of the velocity profile behind both the cylinder becomes similar to that of a single cylinder. The variation of Reynolds number have no appreciable change in C_p distribution for cylinders arranged in tandem.

TABLE OF CONTENTS

	Page
RECOMMENDATION OF THE BOARD OF EXAMINERS	ii
ACKNOWLEDGEMENT	iii
ABSTRACT	iv
TABLE OF CONTENTS	v
LIST OF FIGURES	vii
LIST OF TABLES	x
LIST OF PLATES	xi
NOMENCLATURE	xii
CHAPTER I : INTRODUCTION	1
1.1 Motivation for the study	2
1.2 Aim of the study	2
1.3 Scope of the thesis	3
CHAPTER II : LITERATURE REVIEW	5
CHAPTER III: EXPERIMENTAL SET-UP AND PROCEDURE	13
3.1 The wind tunnel	13
3.2 The test section	15
3.3 The cylinders	16
3.4 Experimental procedure	17
3.4.1 Single cylinder	17
3.4.2 Cylinders in tandem	18
3.4.3 Pressure and velocity measurements.	18
3.5 Uncertainties in the measurements	19

CHAPTER IV :	RESULTS AND DISCUSSIONS	20
4.1	Single cylinder	20
4.2	Cylinders in tandem	22
4.3	Effect of Reynolds number	26
4.4	Blockage correction	27
CHAPTER V :	CONCLUSIONS AND RECOMMENDATIONS	29
5.1	Conclusions.....	29
5.2	Recommendations.....	30
REFERENCES	32
APPENDICES	40
APPENDIX - A :	Determination of Coefficient	41
APPENDIX - B :	Uncertainty analysis	44
FIGURES	50
PLATES	85

LIST OF FIGURES

	Page
3.1 Schematic diagram of the wind tunnel	51
3.2 Perspex vertical side wall of the test section	52
3.3 Perspex and wooden vertical wall side	53
3.4 Sectional view of a specimen square cylinder	54
3.5 The arrangements of tapping points on adjacent side	55
3.6 Velocity distribution in upstream side of the test section.....	56
3.7 Calibrated Micromanometer against U-type manometer	57
4.1 Comparison of C_p -distribution on a square cylinder.	58
4.2 Velocity distribution in a two dimensional wake behind a square cylinder	59
4.3 Mean velocity distribution in wake behind square cylinder	60
4.4 Comparison of drag co-efficient of two tandem square cylinders for different Reynolds number	61
4.5 Variation of drag and lift forces on the surface of two tandem square cylinders due to change in inter spacing at Reynolds number of 2.5×10^4	62
4.6 Variation of drag and lift forces on the surface of two tandem square cylinders due to change in inter spacing at Reynolds number of 4.7×10^4	63
4.7 Variation of drag and lift forces on the surface of two tandem square cylinders due to change in inter spacing at Reynolds number of 6.5×10^4	64
4.8 Mean pressure distribution around two square cylinders for $L/D=1.5$ at Reynolds number of 2.5×10^4	65

4.9	Mean pressure distribution around two square cylinders for $L/D=4.0$ at Reynolds number of 2.5×10^4	66
4.10	Mean pressure distribution around two square cylinders for $L/D 8.75$ at Reynolds number of 2.5×10^4	67
4.11	Effect of L/D on C_p distribution around upstream cylinder with Reynolds number of 2.5×10^4	68
4.12	Effect of L/D on C_p distribution around upstream cylinder with Reynolds number of 4.7×10^4	69
4.13	Effect of L/D on C_p distribution around upstream cylinder with Reynolds number of 6.5×10^4	70
4.14	Effect of L/D on C_p distribution around downstream cylinder with Reynolds number of 2.5×10^4	71
4.15	Effect of L/D on C_p distribution around downstream cylinder with Reynolds number of 4.7×10^4	72
4.16	Effect of L/D on C_p distribution around downstream cylinder with Reynolds number of 6.5×10^4	73
4.16 (a)	Comparison of C_p distribution around downstream cylinder with Reynolds number 5.6×10^4	74
4.16 (b)	The nature of flow pattern around square prism.	75
4.17	Mean velocity distribution in wakes behind upstream and downstream square cylinders arranged in tandem for $L/D = 3.5$	76
4.18	Mean velocity distribution in wakes behind upstream and downstream square cylinders arranged in tandem for $L/D = 3.75$	77
4.19	Mean velocity distribution in wakes behind upstream and downstream square cylinders arranged in tandem for $L/D = 4.0$	78
4.20	Mean velocity distribution in wakes behind upstream and downstream square cylinders arranged in tandem for $L/D = 4.25$	79
4.21	Mean velocity distribution in wakes behind upstream and downstream square cylinders arranged in tandem for $L/D = 4.5$	80

4.22	Mean velocity distribution behind upstream cylinder for longitudinal spacing $L/D = 3.5$ to 4.0	81
4.23	Mean velocity distribution behind upstream cylinder for longitudinal spacing $L/D > 4$	82
4.24	Mean velocity distribution behind downstream cylinder for longitudinal spacing $L/D = 3.5$ to 4.5 .	83

LIST OF TABLE

Table	Page
4.1 Variation of drag co-efficient of present and other cases at various Reynolds numbers with different turbulence intensity	84

LIST OF PLATES

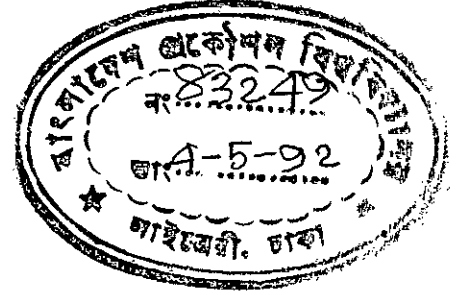
Plates	Page
3.1 Square cylinder with tappings	85
3.2 Co-ordinate measuring machine and pressure transducer.	86
3.3 Square cylinders arranged in tandem in test section	87
3.4 Complete experimental set-up	88

NOMENCLATURE

<u>Symbols</u>	<u>Meaning</u>
A	Front face of the cylinder
b	Half width of the wake
C_D	Drag co-efficient
C_{DF1}	Drag co-efficient of front face of the 1st cylinder.
C_{DF2}	Drag co-efficient of front face of the 2nd cylinder.
C_{DR1}	Drag co-efficient of rear face of the 1st cylinder.
C_{DR2}	Drag co-efficient of rear face of the 2nd cylinder.
C_L	Lift co-efficient.
C_{LB1}	Lift co-efficient of bottom face of 1st cylinder
C_{LB2}	Lift co-efficient of bottom face of 2nd cylinder
C_{LT1}	Lift co-efficient of top face of 1st cylinder
C_{LT2}	Lift co-efficient of top face of 2nd cylinder
C_p	Mean pressure co-efficient
D	Side length of the square cylinder
H	Depth of the test section.
hi	Local pressure head
ho	Stagnation pressure head
hs	Static pressure head
L	Stream-wise centre to centre distance between the two square cylinders.
P	Local static pressure

P_{at}	Atmospheric pressure
P_o	Free steam static pressure.
u	Mean axial velocity
U_o	Free stream velocity
X	Distance from the centre line of the cylinder.
Y	Distance from the bottom surface of test section.
γ	Specific weight of manometer water.
ν	Kinematic viscosity of air.
ρ	Density of air
σ	Turbulence intensity.

Chapter - I



Introduction :

In fluid mechanics the flow around and behind a cylinder is a very important problem from fundamental and applied points of view. Flow past a cylinder is always associated with the separation of flow behind the cylinder incurring large energy losses. Specially in the case of flow past rectangular and square cylinders the separation of flow occurs at the corner of the frontal face and a complex wake is created behind it. So, wind tunnel studies is the only means to investigate the flow phenomena past such cylinders. In this respect study of flow characteristics around square cylinders arranged in tandem would reveal the nature of wind loads which is required for their design . Till now extensive research work has been carried out on isolated bluff bodies only. Study on multiple bluff bodies is a very recent endeavour. Even then very little information is available concerning the flow over square cylinders arranged in tandem although this is a problem of considerable practical significance.

1.1 Motivation For the Study :

While numerous investigations have been made on the flow past single obstacles with various shapes, a few studies have been made on the detailed flow structures associated with complex configuration consisting of multiple obstacles. When more than one bluff body placed at close proximity in a uniform flow, the aerodynamic parameters like drag and lift, pressure distributions and vortex shedding patterns are completely different from the case of a single body.

The problem of predicting the flow patterns around these practical arrangements of bluff bodies can be coped with by developing an understanding of the nature of flow on multiple bluff bodies in close proximity by wind tunnel experiments. With this end in view, the present investigation of pressure distributions around rectangular and square cylinders arranged in tandem and with varying spacing ratios was carried out.

1.2 Aim of the Study :

When more than one bluff body is placed in a uniform flow, the surrounding flow and vortex shedding patterns are different from the case of a single body, because there is interference in the flow by one body on the other depending on the arrangement or spacings of the bodies. In the proposed research, the tandem arrangement of two square cylinders will be studied experimentally.

The prime objectives of the study were :

1. To measure the pressure distribution around the two square cylinders arranged in tandem and observe the effect of varying the spacings between the cylinders.
2. To observe the effect of Reynolds number for each set of spacing of the square cylinders.
3. To measure the drag and lift co-efficient.
4. To study the mean velocity distribution in the wake behind the square cylinders arranged in tandem.

1.3 Scope of the Thesis :

The present research programme covers only the experimental investigation of mean pressure distributions around square cylinders arranged in tandem and mean velocity profiles in the wake. Chapter 2 provides with the brief description of the findings of several researchers in the field of flow over single and multiple bodies. Notable contributions were mainly made by P.W. Bearman [5], B.E. Lee [24], A. Okajima [36], B.J. Vickery [50], Igarashi, T [20] and Zdrankovich [51]. Besides these, findings of several other researchers are also included in this chapter.

In chapter 3, mainly an account of the experimental arrangement and procedure adopted for the investigation are presented. It includes the description of the wind tunnel, the constructional details of the test section and the square cylinders used for the study. The experiment was conducted in the wind tunnel for uniform cross flow keeping the turbulence intensity constant and for three different Reynolds numbers.

Chapter 4 presents the analysis concerning the results of the experiment. The results are presented in graphical form. In few cases the existing experimental results of different researchers are compared with the present one.

Finally, the conclusion which are drawn from the present investigation are given in the chapter 5. This chapter also includes and outlines regarding further research in this field.

Chapter - II

Literature Review

A number of experiments were carried out by several researchers and the effects of flow characteristics around rectangular, square and circular cylinders in tandem were investigated. A brief description of some of the papers related to the present study is given below.

P.W. Bearman and D. M. Truman [5] investigated the base (surface) pressure co-efficient, drag co-efficient and Strouhal number of rectangular cylinder with one face normal to the flow direction. They found that when $d/h = 0.62$, where 'd' is the section depth and 'h' is section width normal to the wind direction, the drag co-efficient was maximum about 2.94. By introducing a splitter plate into the wake region they found that the increased drag effect was completely eliminated. This finding demonstrated that the high drag was associated with the regular shedding of vortices. They also showed that the further the vortices could be persuaded to form away from the body, the higher the base pressure. They suggested that for higher values of d/h (>0.6) the vortices were forced to form further downstream because of the influence of the trailing edge corners.

Robetson, Lin and Rutherford [41] carried out experiments on circular cylinders, spool shaped bodies, cup shaped bodies, square rods and rectangular rods to observe the effect of turbulence on the drag of these bodies. For square rods with their axes parallel to the flow direction it was found the C_D decreased approximately 25% when the turbulence intensity increased from 1% to 10%. Two rectangular rods were used; one had a square cross-section and other had a length (in the free stream direction) to breath ratio of two. The drag was measured with axes of the rectangular rods oriented normal to the free stream direction. It was noted that on the sides of the square rod, the pressure change with a change in turbulence intensity was about the same as for the rear face; but for the rectangular rod, the change in pressure on the side was large, but small on the rear face. They concluded that bodies which have shapes such that reattachment of the flow is not a factor, experience an increase in C_D with increased turbulence intensity. On the other hand bodies for which reattachment or near reattachment of flow occurs with increased turbulence may experience either a decrease or increase in C_D with increased turbulence intensity depending upon the shape of the body.

B.J. Vickery [50] present in his paper the result of the measurements of fluctuating lift and drag on a long square cylinder. He attempted to establish a correlation of lift along the cylinder and the distribution of fluctuating pressure on a cross-section. It was found that the magnitude of the fluctuating lift

was considerably greater than that for a circular cross-section and the spanwise correlation much stronger. It was also reported that the presence of large scale turbulence in the stream had a remarkable influence on both the steady and the fluctuating force. At small angle of attack (less than 10°) turbulence caused a reduction in base pressure and a decrease in fluctuating lift of about 50%.

B.R. Bostock and W.A. Mair [6] studied the pressure distribution and forces on rectangular and D-shaped cylinders placed in two dimensional flow at Reynolds number 1.9×10^5 . It was found that for rectangular cylinders a maximum drag co-efficient, C_D , obtained for $d/h = 0.67$. Reattachments on the sides of the cylinders occurred only for h/d less than 0.35.

E.E. Lee [24] made an elaborate study of effect of turbulence on the base pressure field of a square prism. He presented measurement of the mean and fluctuating pressure on a square cylinder placed in two dimensional uniform and turbulent flow. It was observed that the addition of turbulence to the flow raised the base pressure and reduced the drag of the cylinder. He suggested that this phenomena was attributable to the manner in which the increased turbulence intensity thickenes the shear layers, which causes them to be deflected by the downstream corners of the body and resulted in the downstream movement of the vortex formation region. The strength of the vortex shedding was shown to be reduced as the intensity of the incident turbulence was increased.

Measurement of drag at various angle of attack (0° to 45°) showed that with increased in turbulence level the minimum drag occurred at smaller values of angle of attack.

P.W. Bearman and A.J. Wadcock [7] describes in their paper how the flows around two circular cylinders displaced in a plane normal to the free stream, interact as the two bodies are brought close together. Surface pressure measurement at a Reynolds number of 2.5×10^4 showed the presence of mean repulsive force between the cylinders. At gaps between $1/10$ diameter and one diameter a marked asymmetry in the flow was observed with the two cylinders experiencing different drags and base pressures. The base pressure was found to change from one steady value to another or simply fluctuate between the two extremes. They also showed how mutual interference influence the formation of vortex streets from the two cylinders.

H. Sakamoto and M. Arie [43] collected experimental data on the vortex shedding frequency behind a vertical rectangular prism and vertical circular cylinder attached to a plane wall and immersed in a turbulent boundary layer. They tried to investigate the effect of the aspect ratio (height/width) of these bodies and the boundary layer characteristics on the vortex shedding frequency. Measurements revealed that two types of vortex were performed behind the body, depending on the aspect ratio; they were

the arch type vortex and the Karman type vortex. The arch-type vortex appeared at an aspect ratio less than 2.0 and 2.5 for rectangular and circular cylinders respectively. The Karman type of vortex appeared for the aspect ratio greater than the above values. The whole experiment was conducted at a turbulence level of 0.2% and free stream velocity of 20 m/sec. The aspect ratio was varied between 0.5 to 0.8.

A. Okajima [37] conducted experiments in a wind tunnel and in a water tank on the vortex shedding frequencies of various rectangular cylinders. He presented results that showed how Strouhal number varied with width to height ratio of the cylinders for Reynolds number between 70 and 2×10^4 . He found that there existed a certain range of Reynolds number for the cylinders with the width to height ratios of two and three where flow pattern abruptly changed with a sudden discontinuity in Strouhal number. For Reynolds number below this value, the flow separated at the leading edges, reattached on either the upper or lower surfaces of the cylinder during a period of vortex shedding. Again for Reynolds number beyond it the flow fully detached itself from the cylinder.

R.W. Davis and E.F. Moore [10] carried out a numerical study of vortex shedding from rectangular cylinders. They attempted to present numerical solution for two dimensional time dependent flow about rectangles in finite domains. They investigated the initiation and subsequent development of the vortex shedding phenomena for Reynolds number varying from 100 to 2800. They found

that the properties of these vortices were strongly dependent on the Reynolds number. Lift, drag and Strouhal number were also found to be influenced by Reynolds number.

T. Igarashi [19] reported on the characteristics of flow around two circular cylinders of different diameters arranged in tandem. The Reynolds number defined by the diameter of the first cylinder was varied in the range of 1.3×10^4 to 5.8×10^4 and the longitudinal spacing between the axes of the cylinders in the interval of 0.9 diameter to 4.0 diameters. He discussed difference in the flow separation, jump phenomena and the bistable flow at the critical region for the cases of cylinders with equal and unequal diameters.

M.M. Zdravkovich [51] made an experimental investigation with a smoke visualization technique the laminar wake behind a group of three cylinders. The main characteristics of the interaction between the three cylinders was the appearance of strong sinuous oscillations some distance downstream in the wake, which led to the formation of a new single vortex street. The mechanism of the formation process of this vortex street and the part played in it by the sinuous oscillations is demonstrated by series of photographs. In an interaction between three fully developed vortex streets, some of the rows of vortices crossed and there was an extremely complicated rearrangement of vorticity in the wake. They also found wakes were some-times which were laminar on one side and turbulent on the other.

T. Igarashi and K. Suzuki [21] conducted experimental investigation on the characteristics of the flow around three circular cylinders arranged in line. There were three cases concerned with the behavior of the shear layers separated from the first cylinders on the down stream ones, the first was a case without reattachment, the second was one with reattachment and the third was one rolling up in the front region of the down stream cylinder.

T. Igarashi's [20] experimental investigation was carried out on the characteristics of the flow around four circular cylinders arranged in line. Concerning the behavior of the shear layers separated from the first cylinder to the downstream ones, the flow patterns were classified according to the longitudinal spacing between the axes of the cylinders and Reynolds numbers. Flow characteristics of these patterns were elucidated. The Reynolds numbers corresponding to the reattachments of the shear layers into the second cylinder were obtained. The flow characteristics around the down stream cylinders changed drastically in this transition region. Thereby, a bistable flow and a hysteresis phenomenon emerged.

H. Masanori and A. Sakurai [27] explain in their paper the wake characteristics of group of normal flat plates, consisting of two, three or four plates placed by side with slits in between to the normal flow direction. They found that when the ratio of the slit width to the plate width (slit ratio) of a row of flat plate

is less the flows through the gaps were biased either upward or downward in a stable way, leading to multiple, stable flow pattern for single slit ratio value. The plates on the biased side showed high drag and regular vortex shedding, while these on the unbiased side showed the opposite. They suggested that the origin of biasing is strongly related to the vortex shedding of each plate of a row.

S.C. Luo and T.C. Teng [52] reports on the measurements of aerodynamic forces on a square cylinder which was downstream to an identical cylinder. They considered both tandem and staggered arrangements of the cylinders. They showed that when the two cylinders were in tandem formation a critical spacing equal to about four times the side length D of the square cylinder existed. Also they found that when the two cylinders were in staggered formation, the lift force that act on the down stream cylinder can be either positive or negative.

The literature survey reveals that numerous papers have been published in the area of flow past one or more circular and rectangular cylinders. While fairly extensive investigation had been carried out in the area of flow past a single square cylinder, much less has been done in the field of flow past two or more. The present investigation is devoted to the study of flow past two square cylinders arranged in tandem.

Chapter - III

EXPERIMENTAL SET-UP AND PROCEDURE

The investigation of flow characteristics around square cylinders arranged in tandem was carried out in a subsonic wind tunnel. Mean pressure distribution around the rectangular cylinders placed normal to the approaching uniform flow was measured with the help of a digital manometer. The following section describe in detail the experimental set-up and technique adopted for the investigation.

3.1 The Wind Tunnel :

The experiment was carried out in an open circuit subsonic wind tunnel which was 16.15 m (53 ft) long with a test section of 0.46 m (1.5 ft) x 0.46 m (1.5 ft) cross-section. Fig . . . shows the wind tunnel and its different sections.

The wind tunnel contains successive section such as a filter-cum settling chamber a bell mouth entry, an eddy breaker, a flow straightener, a uniform perspex upstream section, test section, diverging section, two counter rotary axial flow fans, flow controlling valve and a silencer. The set up of the wind tunnel was situated at a constant height from the floor with its central longitudinal axis. The filter-cum settling chamber was made of a

rectangular wooden frame measuring 2540 mm x 1524 mm x 2134 mm covered with 25.4 mm thick foam sheets. The outer surface of the settling chamber was covered with a cloth in order to keep the foam clean and to prevent external dust. This chamber immunized the flow inside the tunnel against all outside disturbance and maintain uniform flow into the duct free from foreign particles.

The bell mouth entry nozzle, made of 18 SWG black sheets was 1180 mm long with a contraction ratio of 10:3. Wire net with 2 holes/cm was fitted at the entrance of the nozzle to act as the primary eddy breaker. A honey comb was made by a stack of 25.4 mm diameter and 150 mm long p.v.c. pipes. It was situated after the nozzle. For produce stable and more uniform flow, both ends of the honey comb section was guarded by wire net with 2 holes/cm.

The diverging section of the wind tunnel, made of 15 SWG black sheet, was 3962 mm long. The angle of divergence is 6° which was done with a view to minimize expansion loss and reduce the possibility of the separation. A foam made isolator was placed between the fan unit and the diverging section of the wind tunnel to prevent transmission of vibration towards the main test section.

The flow was produced by a two stage contra rotating axial flow fans (Woods of Clochester Ltd England type 38 JTE) of capacity

14.2 m³/s (30,000 cfm) at a head of 152 mm of water and at 1475 rpm. The butterfly valve was used to control the flow. A screw thread mechanism was used to actuate the valve.

Finally the silencer 2743 mm long and 3735 mm diameter was fitted at the end of the tunnel to reduce the noise of the system.

3.2 The Test Section :

The test section was made by the combination of wood, plywood and perspex sheet. The constructional views of this section are shown in figs. 3.2 and 3.3. The length of the test section was 1522 mm, breadth and height 457 mm x 457 mm and it was adjacent to the 762 mm upstream perspex section. The top and bottom of the test section was made of plywood. As shown in the figure one side wall was made in such a way as to fulfil the requirements of the experimental procedure. A 22 mm wide and 483 mm long slot was made at the mid plane of the test section so as to enable longitudinal movement of the centrally mounted cylinders. Also a square hole of dimension 127 mm x 127 mm was provided at the end of the slot so that the square cylinders could be mounted in the test section through this hole. A similar slot was provided on the opposite side wall which was made of 9 mm perspex sheet and grooves 16 mm x 483 mm. The perspex wall was provided for observation of the probes and for setting the cylinders properly during the experiment.

3.3 The Cylinders :

The two square cylinders 457 mm long were made of perspex sheet. The dimension of each cylinder was 50 mm x 50 mm, 4 mm thick perspex sheet was used to make the cylinders. One end was closed by inserting a solid wooden block and the other end by inserting another wooden hollow block with (22.0 mm) through hole. On either side of the cylinders there were 28 mm long projected circular portion in order to mount the cylinder as shown in fig. 3.4. The extreme end of the 15 mm diameter projected portion of the cylinder was given a square shape and allowed to pass through the identical rectangular hole. This provision was needed to maintain for tandem orientation of the cylinders. Each square cylinder was tapped on four sides to measure pressure distribution. Nine pressure tapings were made on each side of the cylinder.

As shown in fig. 3.5 the tapings were placed in an inclined sectional plane for making easy connections. It was assumed that for two dimensional flow, such placement of tapping would not effect the results.

To make the pressure tapings 1.5 mm holes were made on each surface of the cylinder plates. Then 10mm long copper tube were press fitted to the tapping holes and sealed with "Arreldide" gum. The exposed end of the copper tubes were connected with the flexible plastic tubes of 1.6mm diameter which were used to connect the tapings to the limbs of a digital manometer.

3.4 Experimental Procedure :

The test was conducted in two phases. In the first phase pressure distribution on a single cylinder was made. In the second phase pressure distribution around two square cylinder for various interspacing was measured. Three sets of measurements were taken for Reynolds number such as 2.5×10^4 , 4.7×10^4 and 6.5×10^4 for different L/D ratio ranging from 1.5 to 3.75 for each set. The mean flow velocity in the test section for these three sets were 7.56 m/sec, 13.94 m/sec and 18.95 m/sec respectively. The turbulence intensity of the tunnel was approximately 0.17% [53].

Before measuring the pressure distribution the mean velocity was measured in a vertical plane 60 cm upstream from the cylinders by means of a pitot static tube connected to a digital manometer. The measured velocity distribution was uniform which can be seen from the fig. 3.6. One may also observe from the figure that there is a velocity gradient within 40 mm from the tunnel surfaces.

3.4.1 Single Cylinder :

The square cylinder was mounted centrally in horizontal plane at a distance of 1.45 m (57 inch) from the end of the throat of the entry nozzle. The 50 mm face of the cylinder was oriented normal to the flow direction. The mean pressure distribution on the body was recorded by means of a digital manometer. A pitot static tube for

indicating the free stream velocity and pressure was placed centrally and 60 cm ahead from the centre of the cylinder.

3.4.2 Cylinders in Tandem :

Two square cylinders were placed in the tandem position. Initially the cylinders were mounted in such a way that the centre to centre distance was $L/D = 1.5$. For Reynolds number 2.5×10^4 pressure distribution around the cylinders were measured for seven set of interspacings. Also mean velocity in the wake of both the upstream and downstream cylinders were measured for each set of interspacing. Similar experiment was also done for Reynolds number of 4.7×10^4 and 6.5×10^4 .

3.4.3 Pressure and velocity measurements :

a. Digital manometer :

The digital Micromanometer used was manufactured by furness controls limited, Bexhill England. Pressure reading upto 0.001 mm H_2O could be taken by the micromenometer. The instrument was calibrated against a U-tube manometer with was as the manometer liquid. The calibrated curve is shown in figure 3.7.

b. Traversing Mechanism :

The pitot static tube was traversed in the air stream by Mitutoyo co-ordinate Measuring Machine (type CX 652 code 198402)

with ranges X co-ordinate 800 mm, Y co-ordinate 500 mm and Z co-ordinate 400 mm. The mechanism was actuated by a wheel through a rack and pinion arrangement and by the help of it a position was fixed up to an accuracy of 0.01 mm.

In order to prevent undue vibration of the sensing probe, the pitot-static tube was supported by an Aluminium rod of diameter 10 mm. The rod was rigidly fixed to the holder which was again fixed with the traversing gear. The sensing point was kept 15.24 cm beyond the end of the rod to ensure that no major disturbances occurred near the sensing point of the pitot tube by the presence of the rod.

3.4.4 Uncertainty in the Measurements :

Error are introduced during measurement due to atmospheric changes, measuring instruments, probe setting etc. An uncertainty analysis is made for different measured parameters which is illustrated. It is found that the uncertainty in surface static pressure measurements is 0.00098% for $Re = 6.5 \times 10^4$. For different Reynolds number the uncertainties in velocity measurements are different. It was found that for Reynolds number 5.04×10^4 uncertainty in velocity measurements were 2.82%.

Chapter - IV

Results and Discussion

This chapter is devoted to the analysis of the results obtained from the investigation of flow on square cylinders arranged in tandem. The experiment was conducted for three different Reynolds number such as 2.5×10^4 , 4.7×10^4 and 6.5×10^4 . Effect of interspacing between the cylinders was observed by changing the ratio L/D . In addition comparative study of the existing research works and the present investigation are presented.

4.1 Single Cylinder :

The distribution of mean pressure co-efficient for the square cylinder has been presented in fig. 4.1. For this case the Reynolds number was 6.05×10^4 and turbulence intensity was 0.17% [53].

The result of the present experiment is compared with that of Lee (24), A.C. Mandal (28) and Pocha [24] as shown in the figure. These experiments were done at different turbulence intensity. This parameter has a great influence on the surface pressure distribution as may be seen from the figure, except at the front face. The C_p distribution at the front face shows that it is nearly

independent of turbulence intensity and a stagnation point is established at the middle of the face. At other faces the C_p distribution for smaller turbulence intensity cases (for T.I <5%) has more or less same nature and they are within 7% of deviation. But for 12.5% turbulence intensity case the variation is quite significant.

Table 4.1 shows the co-efficient of drag C_D of present and other cases at various Reynolds numbers with different turbulence intensity. It is seen that the value of the drag co-efficient is highest for the present case. However, it can be noted that the drag co-efficient becomes smaller with the increase in turbulence intensity as it is mentioned by Roberson et al [41].

Dimensionless velocity distribution in a two dimensional wake behind a square cylinder is shown in fig.4.2 to examine self preservation of flow. Here measured values have been compared with the theoretical curve shown in figure. It is seen that there is good agreement between them. Fig. 4.3 shows the mean velocity distribution in wake behind a single square cylinder. It is seen that the spread of the wake increases as distance from the body is increased and the difference between the velocity in the wake and that outside become smaller. Such a spread of a wake is logical from the view point of energy transfer to the wake from the surrounding.

4.2 Cylinders in Tandem :

Fig. 4.4 shows the variation of drag co-efficient with interspacing of the square cylinder arranged in tandem and also comparison is made with similar curve is obtained by Yujichya et al [55] and Luo and Teng [52]. It is seen that for the downstream cylinder negative drag exists for $L/D < 4$. However when $L/D > 4$ positive drag occurs. The explanation to the above observation is that when $L/D < 4$ the boundary layers that separate from the upstream cylinder reattach on to the downstream cylinder and a region of slow moving fluid is formed which is bounded by the shear layers and the two cylinders. The bounded region is at a pressure that is lower than the wake pressure of the downstream cylinder and hence the latter is subjected to a negative drag force or thrust. This fact is supported by pressure distributions as shown in figure 4.8, 4.9 and 4.10. In this case only the downstream cylinder is shedding vortices [52]. For $L/D > 4$, both cylinders are shedding vortices [52], the pressure distribution at the rear side of the downstream cylinder is lower than the front pressure and thus subjected to a positive drag.

Fig. 4.5 shows the variation of drag force and lift force on the surface of two tandem square cylinders due to change in interspacing at Reynolds number 2.5×10^4 . It can be seen from the figure that the lift force on the top and bottom surfaces of the

cylinders is same, hence no net lift force act on the cylinder. Similar occurrence is observed in figs. 4.6 and 4.7 for $Re = 4.7 \times 10^4$ and 5.5×10^4 .

Fig. 4.8 to 4.10 show the mean pressure distribution around two tandem square cylinders at Reynolds number 2.5×10^4 for different interspacing. On the upstream cylinder stagnation point exist at the mid point of the front surface. For the downstream cylinder no such stagnation point is observed on the front surface. Instead very high negative pressure is observed on the front surface. However with increasing interspacing the C_p values on the front surface of the downstream cylinder become less negative. The pressure distribution on the bottom and top surfaces of the square cylinders are more or less uniform for all spacings. Also the pressure distribution on the back surfaces reveal a similar trend.

Fig. 4.11 to 4.13 shows the effect of L/D on C_p distribution around upstream cylinder. It can be observed that on the top and bottom surface the pressure distribution is uniform for all spacings but beyond $L/D = 4$, the C_p values become more negative. A similar occurrence is observed for the back surface also.

Fig. 4.14 to 4.16 shows the effect of L/D on the C_p distribution around the downstream cylinders. In both figures it is observed that for $L/D < 4$ the pressure on the front surface is much lower than the wake pressure of the down stream cylinder. However beyond $L/D = 4$ the front surface pressure is higher than that of

the back surface pressure. It is noticed that when $L/D < 4$ the pressure on the rear face of the downstream cylinder increases (become less negative) with an increased L/D .

Fig. 4.16(a) shows the comparison of C_p distribution around downstream cylinder with present research Reynolds number 6.5×10^4 . It is observed comparison is made with similar curve is obtained.

In the case of a sharp edged body like a square cylinder the separation points are fixed at the leading edges (corners of the front face) and thus the shear layers originating at the front corner curve outward and these appear the formation of familiar vortex shedding in the wake region behind the body. This is illustrated in fig. 4.16 (b). The free shear layers are basically unstable and roll up to form discrete vortices. The growing vortices draw in fluid from the base region and it is suggested that it is this continual entrainment process that sustain the low negative pressure. In fact the magnitude of the negative pressure is determined almost solely by the manner in which the shear layers leave the body and roll up to form discrete vortices. Thus a low base pressure is associated with vortex formation close to the body while a high base (less negative value) is caused by vortex formation further away. In the present case for $L/D < 4$ the presence of the downstream cylinder close to the upstream cylinder causes the separated boundary layers of the upstream cylinder to be deflected further downstream cylinder and as a result the vortices

are formed further away from the rear face of the downstream cylinder. This results in an increase in pressures on the rear face of both in the upstream and downstream cylinder as shown in figs. 4.111 and 4.13.

Fig. 4.17 to 4.21 show the mean velocity distribution in the wakes behind up and down stream cylinders arranged in tandem for different spacings. It can be seen from the figures that for spacing up to $L/D = 4$ the velocity profiles in the wake of the upstream cylinder are similar. It can be seen that the velocity defect is considerably large behind the upstream cylinder for $L/D < 4$. Also there is not much change in the half width. However for $L/D > 4$ the velocity defect behind the upstream cylinder becomes smaller and gradually decreases with increase in longitudinal distance. In fact the shape of the profile becomes more or less similar to that of single cylinder. For the downstream cylinder however the nature of the velocity profile is more or less similar to that of a single cylinder for all longitudinal spacings.

Fig. 4.22 shows the mean velocity distribution behind upstream cylinder for longitudinal spacings $L/D = 3.5$ to 4.0 . It can be seen that the width of the velocity profile does not change through out the length of the velocity defect and it assumes a rectangular shape rather than a triangular shape.

Fig. 4.23 shows the velocity distribution behind upstream cylinder for longitudinal spacing $L/D > 4$ and fig. 4.24 shows the

same behind downstream cylinder for longitudinal spacing $L/D = 3.5$ to 4.5. It is observed from both the figures that the shape of the velocity profile is similar to that of a single cylinder.

4.3 Effect of Reynolds Number :

Besides at extremely low Reynolds number it has been shown by tests carried over a wide range of Reynolds number that the flow pattern around sharp edged body is relatively insensitive to Reynolds number. This is because the position of the flow separation are fixed by the sharp edges. R.W. Davis [10] showed that for Reynolds number less than 1000 the flow around rectangular cylinders was strongly dependent on Reynolds number. In case of extremely low Reynolds number flow reattachment occurs immediately after separation from the front corner and finally it separates at the trailing edges. With an increase of Reynolds number, flow separation occurs at the leading edges and hence forth flow pattern becomes independent of Reynolds number. However, in case of reattachment appearing for the change of tandem position of square cylinder, the effect of Reynolds number may not be ignored. The nature of pressure distribution around the square cylinder for two different Reynolds numbers shown in fig. 4.16 (a) demonstrates that flow pattern is not effected by Reynolds number.

4.4 Blockage Correction :

The presence of a body in the wind tunnel test section reduces the flow area and thereby increases the velocity of air as it flows around the body. This increase of velocity due to the presence of the body is called solid blocking. The wake behind a body has a mean velocity lower than the free stream. According to the law of continuity, the velocity outside the wake must be higher than free stream so that a constant volume of fluid may pass through the tunnel test section. According to Bernoulli's principle this increase in speed is balanced by a decrease in static pressure of the main stream. Consequently, since the static pressure within the wake is governed by that of the steady airstream immediately adjacent to the boundary of the wake, the static pressure at back surface of the body ends to be less than it would be if the air stream were unconfined. Due to this wake blocking and solid blocking, blockage corrections are required to obtain accurate values of nondimensional coefficients. Investigation of this effect has shown that sufficient accuracy in results are obtained for models occupying less than 10% of the tunnel working section area [56].

The total solid and blockage corrections are summed to get the total blockage corrections. According to Pope and Harper [39] the total blockage corrections to C_p would be approximately of the order of half times the blockage percentage. In the present study

maximum blockage percentage was around 11% for the single cylinder. No blockage corrections were made because the corrections needed are small and also any corrections would make the co-efficient less conservative (i.e. the value of C_p would be more positive).

Chapter - V

Conclusions and Recommendations

This chapter summaries the achievements of the present experimental investigation and suggests the scope of extension and development of the present study. The tandem parameters used in the present study is comparatively large from that used by the previous researchers. The effect of flow characteristics around square cylinders in tandem, pressure co-efficient, drag co-efficient and other parameters are analysed.

5.1 Conclusions :

1. $L/D = 4$ is the critical spacing which effects the pressure distribution and aerodynamic forces on both cylinder.
2. The presence of the downstream cylinder increases (becomes less negative) the magnitude of C_p on the top, back and bottom surfaces of the upstream cylinder for $L/D < 4$.
3. The change of Reynolds number have no appreciable change in the C_p -distribution for the cylinders arranged in tandem.

4. For $L/D < 4$ the pressure on the front surface of the downstream cylinder is much lower than the wake pressure of the same cylinder. Beyond $L/D = 4$ the front surface pressure rises above that of the back surface pressure.
5. When $L/D < 4$ the down stream cylinder is subjected to negative drag. And at $L/D > 4$ positive drag occurs.
6. The width of the velocity profile does not change throughout the length of the velocity defect and it assumes a rectangular shape rather than a triangular shape when $L/D < 4$.
7. Half width increases with increases of axial distance.

5.2 Recommendations :

1. The same experiment can be done with flow visualization technique to get a better understanding about the formation of wakes and vortex shedding pattern.
2. Experiments can be carried out with various turbulence intensities.
3. Further investigation can be carried out around the critical spacing $L/D = 4$ for square cylinders arranged in tandem.
4. The study of flow around tandem square cylinders at different angles of attack may be done.

5. Similar experiment can be carried out on rectangular cylinders.
6. The effect of Reynolds number on cylinders arranged in tandem with varying side ratios may be investigated.

REFERENCES

References

1. Aiba, S., Ota, T. and Tsuchida, H., "Heat transfer tubes closely spaced in an in lined bank", International Journal heat and mass transfer, Vol. 23, 1980, pp. 311-319.
2. Achenback, E., " Distribution of local pressure and skin friction around a circular cylinder in cross flow up to $Re = 5 \times 10^6$ ", Journal of fluid Mechanics, Vol. 34, 1968, pp. 625-639.
3. Bradshaw, P., "The effect of wind tunnel screens on nominally two dimensional mechanics, vol. 22, part 4, 1965, pp. 679-687.
4. Baines, W.D., "Effect of velocity distribution on wind loads and flow patterns on buildings", Proceeding of a sumposium on wind effects on buildings and structures, U.K., 1963, pp. 197-225.
5. Bearman, P.W. and Trueman, D. M., "An investigation of the flow around rectangular cylinders", The aeronautical quarterly, Vol. 23, 1972, pp. 228-237.
6. Bostock, B.R. and Mair, W. A., "Pressure distributions and forces on rectangular and D-shaped cylinder", The aeronautical quarterly, Vol. 23, 1972, pp. 1-5.
7. Bearman, P.W. and Wadcock, A. J., "The interaction between a pair of circular cylinders normal to a stream", Journal of fluid mechanics, Vol. 61, 1973, pp. 499-511.
8. Castro, I. P. and Robins, A.G., "The flow around a surface mounted cube in uniform and turbulent streams", Journal of fluid mechanics, Vol. 79, 1977, pp. 307-335.

9. Carl, E. Pearson, "A computational method for viscous flow problems", J.F.M., Vol. 25, 1965, pp. 611-622.
10. Davies, R.W. and Moore E.F., "A numerical study of vortex shedding from rectangles", Journal of fluid mechanics, Vol. 116, 1982, pp. 475-506.
11. Frank, N., "Model law and experimental technique for determination of wind loads on buildings," Proceeding of the 1st international conference on wind effect on building structures, Teddington, London, 1963, pp. 181-189.
12. Frederick, H. A., and Richard, E.K., "The formation of vortex streets", Journal of fluid mechanics, vol. 13, 1962, pp. 1-20.
13. Gandemer, J., "Wind environment around buildings aerodynamics concepts", Proceedings of the 4th international conference on wind effects on buildings and structures, London, U.K., 1975, pp. 423-432.
14. Gerrard, J. H., "The mechanics of the formation region of vortices behind bluff bodies", Journal of fluid mechanics, Vol. 25, 1966, pp. 431-413.
15. Hayachi, M., Akirasakurai and Yujishya, "Wake interference of a row of normal flat plates arranged side by side in a uniform flow", Journal of fluid mechanics, Vol. 164, 1986, pp. 1-25.
16. Hnot, J.P., Rey, C. and Arby, H., "Experimental analysis of the pressure field induced on a square cylinder by a turbulent flow", Journal of fluid mechnics, Vol. 162, 1986, pp. 283-298.
17. Honji, H., "Formation of reversed flow bubble in the time mean wake of a row of ciruclar cylinders", Journal of the physical society of Japan, Vol. 35, No. 5, November, 1973, pp. 1533-1536.

18. Jonji, H., "Viscous flow past a group of circular cylinders", Journal of the physical society of Japan, Vol. 34, no. 3, March, 1973, pp. 821-828.
19. Igarashi, T., "Characteristics of a flow around two circular cylinders of different diameters arranged in Tandem", Bulletin of the JSME, Vol. 25, no. 201, March, 1982, pp. 349-357.
20. Igarashi, T., "Characteristics of the flow around four circular cylinders arranged in line", Bulletin of JSME, Vol. 29, no. 249, March, 1986, pp. 751-757.
21. Igarashi, T. and Suzuki, K., "Characteristics of the flow around three circular cylinders arranged in line", Bulletin of JSME, Vol. 27, no. 233, November, 1984, pp. 2397-2404.
22. Koeming, K. and Roshko, A., "An experiment study of geometrical effect on the drag and flow field of two bluff bodies separated by a gap", Journal of fluid mechanics, Vol. 156, 1985, pp. 167-204.
23. Kostić Z. G. and Oka, S. N., "Fluid flow and heat transfer with two cylinders in cross flow", International Journal heat & mass transfer, Vol. 15, 1972, pp. 279-299.
24. Lee, B.E., "The effect of turbulence on the surface pressure field of a square prism", Journal of fluid mechanics, Vol. 69, 1975, pp. 263-282.
25. Lane Vile, A. and Parkinson, G.V., "Effect of turbulence on galloping of bluff cylinders", Proceedings of the 3rd international conference on wind effects on buildings and structures, Tokyo, Japan, 1971, pp. 787-797.
26. Lawson, T.V., "Wind effects on buildings", Vol. 1, Applied science publisher Ltd., London, 1980.

27. Masanori, H. and Sakurai, A., "Wake interference of a row of normal flat plates arranged side by side in a uniform flow", *Journal of fluid mechanics*, Vol. 164, 1986, pp. 1-25.
28. Mandal, A.C., "A study of wind effects on square cylinders," M.Sc. Thesis, BUET, 1979.
29. Mair, W. A., and Maull, D. J., "Aerodynamic behaviour of bodies in the wakes of other bodies", *Phil Royal Society of London*, A. 269, 1971, pp. 425-437.
30. Modi, V. J. and EL-Sherbiny, S., "Wall confinement effect on bluff bodies in turbulent flows", *Proceedings of the 4th international conference on wind effect on buildings and structures*, London U.K., 1975, pp. 121-132.
31. Mandal, A.C., Islam, O., "A study of wind effect on a group of square cylinders with variable longitudinal spacing", *Mechanical engineering research bulletin*, Vol. 3, No.1, 1980.
32. McLaren, F. G., Sherratt, A.F.C. and Morton, A.S. "Effect of free stream turbulence on drag coefficient of bluff sharp-edged cylinders", *Nature*, Vol. 224, No. 5222, No. 29, 1969, pp.908-909.
33. Nakamura, Y. and Ohya, Y., "The effect of turbulence on the mean flow past square rods", *Journal of fluid mechanics*, Vol. 137, 1983, pp. 331-345.
34. Newberry, C.W., "The measurement of wind pressure on tall buildings and structures", *proceedings of the 1st international conference on wind effect of buildings and structures*, Teddington, U.K., pp. 113-149.

35. Nakamura, Y. and Yujishya, 'Vortex steadding from square prisms in smooth and turbulent flows", Journal of fluid mechnics, Vol. 164, 1986, pp. 77-89.
36. Okajima, A., "Flow around two tandem circular cylinders at very high Reynolds numbers", Bulletin of the JSME, Vol.22, no. 166, April 1979, pp. 504-511.
37. Okajima, A., "Strouhal numbers of rectangular cylinders", Journal of fluid mechnics, Vol 123, 1982, pp. 379-398.
38. Parkinson, G.V. and Modi, V.J., "Recent research on wind effect on bluff two dimensional bodies", Proceedings of international research seminar, Wind effects on buildings and structures, Ottawa, Candda, 1967, pp. 485-514.
39. Pope, A. and Harper, J.J., Low speed wind turnnel testing, John willey and Sons, New York, 1966.
40. Roshko, A., "Experiments on the flow past a circular cylinder at very high Reynolds number", Journal of fluid mechanics, Vol. 10, 1961, pp. 345-356.
41. Roberson, J.A., Lin, Chiyu and Rutherford, G.S., "Turbulence effects on drag of sharp-edged bodies", Journal of hydrolics Division, Vol. 98, No. HY7, July, 1972, pp. 1187-1201.
42. Robertson, J. M., "Pressure field at reattachment of separated flows", Proceedings of the 2nd U.S. national conference on wind engineering research, June 22-25, 1975, Colorado.
43. Sakamoto, H. and Arie, M., "Vortex shedding from a rectangular prism and a circular cylinder placed vertically in turbulent boundary layer", Journal of fluid mechanics, Vol. 126, 1983, pp. 147-165.

44. Schlickting, H., Boundary layer theory, Seventh edition.
45. Simiu, E. and Scanlan, R.H., Wind effect son structures : An introduction to wind engineering John Willey and sons, New York.
46. Williamson, C.H.K., "Evolution of a single wake behind a pair of bluff bodies", Journal of fluid mechanics, Vol. 159, 1985, pp. 1-18.
47. West, G.S. and Apelt, C.J., "The effect of tunnel blockage and aspect ratio on the mean flow past a circular cylinder with Reynolds number between 10^4 to 10^5 ", Journal of fluid mechanics, 13 May 1981.
48. Whitbread, R.E., "Model simulation of wind effects on structures," Proceedings of the 1st international conference on wind effects on buildings and structures, U.K., 1963, pp. 283-301.
49. Wiren, B.G., "A wind tunnel study of wind velocities", Proceedings of the 4th international conference on wind effects on buildings and structures, London, U.K., 1975, pp. 465-475.
50. Vickery, B.J., "Fluctuating lift and drag on a long cylinder of square cross-section in a smooth and in a turbulent stream", Journal of fluid mechanics, Vol. 25, part. 3, 1966, pp. 481-491.
51. Zdravkivich, M.M., "Smoke observation of the wake of a group of three cylinders at low Reynolds number", Journal of Fluid Mechanics, Vol. 322, 1968, pp. 339-351.

52. Luo S.C. and Teng T.C., "Aerodynamic forces on a square section cylinder that is down-stream to an identical cylinder", Aeronautical Journal, June/July, 1990.
53. Altaf Hasan, "Study of turbulent boundary layer in a step change from smooth to rough surface", M.Sc. Thesis, BUET, 1984.
54. Klime S. J. and McClintock, "Describing uncertainties in single sample experiments", Mechanical Engineering Journal, January, 1953.
55. Yuji Ohya, Atsushi Okajima and Masanrvi Hayashi, " Wake interference and vortex shedding", Encyclopedia of Fluid Mechanics (Ed. NP. Chermisinoff), Gulf Publishing Co., Vol. 8, Chapter-10, pp. 323-388.
56. Islam, O. Part-1 : Possibilities of studies of wind effect in Bangladesh, Department of Aeronautical and Mechanical Engineering, University of Salford, U.K., July, 1976.

APPENDICES

APPENDIX - A

Determination of Lift and Drag Co-efficients :

The section of the cylinder shown in the above figure is divided horizontally and vertically into nine strips of width are shown with a tapping point at the midpoint of each strip.

Now Drag force on the front face

$$F_{D_f} = \gamma_w [P_1 \partial x_1 + P_2 \partial x_2 + \dots + P_9 \partial x_9]$$

$$= \gamma_w \left[\sum_{i=1}^9 P_i \partial x_i \right]$$

$$F_{D_r} = \gamma_w \left[\sum_{i=19}^{27} P_i \partial x_i \right] \quad (\text{For rear face})$$

Similarly vertical force on the top surface.

$$F_{V_t} = \gamma_w \sum_{i=10}^{18} P_i \partial x_i$$

$$F_{V_b} = \gamma_w \sum_{i=28}^{36} P_i \partial x_i \quad (\text{For bottom face})$$

∴ Drag co-efficient

$$C_D = \frac{(F_{D_f} - F_{D_r})}{\frac{1}{2} \rho A U_0^2}$$

$$= \frac{\gamma_w \left\{ \sum_{i=1}^9 P_i \partial x_i - \sum_{i=19}^{27} P_i \partial x_i \right\}}{\frac{1}{2} \rho A U_0^2}$$

$$= \frac{\sum_{i=1}^9 h_i \partial x_i - \sum_{i=19}^{27} h_i \partial x_i}{A(h_s - h_o)}$$

Similarly lift co-efficient

$$C_L = \frac{\sum_{i=28}^{36} h_i \partial x_i - \sum_{i=10}^{18} h_i \partial x_i}{A(h_s - h_o)}$$

Pressure co-efficient

$$C_p = (P - P_o) / \frac{1}{2} \rho U_0^2$$

$$\text{Now } \frac{1}{2} \rho U_0^2 = \gamma_w (h_s - h_0)$$

$$(P_0 - P_{at}) = \gamma_w (h_0 - \frac{h}{\rho U_0^2})$$

$$(P - P_{at}) = \gamma_w h$$

$$P - P_0 = \gamma_w (h - h_0)$$

$$\therefore C_p = \frac{\gamma_w (h - h_0)}{\gamma_w (h_s - h_0)}$$

$$= \frac{(h_i - h_0)}{(h_s - h_0)}$$

APPENDIX - B

Uncertainty Analysis

Errors are introduced during measurements, due to atmospheric changes, measuring instruments, probe setting etc. Uncertainties thus may have crept into the measurements of pressure and it is analysed in the way suggested by Kline and McClintock (54).

Uncertainty for pressure Measurement :

$$\text{If } u = f(\alpha_1, \alpha_2, \dots, \alpha_n) \quad (1)$$

$$\text{Then the mean } \mu u = f(\bar{\alpha}_1, \bar{\alpha}_2, \dots, \bar{\alpha}_n) \quad (2)$$

$$\text{and the variance } \sigma u^2 = \sum \left(\frac{\sigma u}{\sigma \alpha_i} \right)^2 \sigma \alpha_i \quad (3)$$

In terms of objective co-efficient of variance

$$\delta u = \frac{\sigma u^2}{\mu u^2} = \sum \left(\frac{\partial \delta u}{\partial \alpha} \cdot \frac{\alpha_i}{\mu u} \right)^2 \left(\frac{\sigma \alpha_i}{\alpha_i} \right)^2 \approx \sum_{i=1}^n \left(\frac{\delta u}{\delta \alpha_i} \cdot \frac{\alpha_i}{\mu u} \right)^2 \delta^2 \alpha_i \quad (4)$$

where δu is the co-efficient of variance and $\delta \alpha_i$ is the co-efficient of variance of free variables α_i .

It may be noted that co-efficient of variance is often used as measure of uncertainties.

The wall static pressure measured from the surface tapping were the gage pressure below atmospheric pressure. If P be the absolute static pressure and P_a be the atmospheric pressure, then the recorded pressure be

$$P_r = P_a - P \quad (5)$$

and the absolute static pressure

$$P = P_a - P_r \quad (6)$$

The recorded pressure is nothing but $\gamma_w h_w$

So that

$$P = P_a - \gamma_w h_w = P_a - \gamma_w h_w / 1000 \quad (7)$$

where h_w is in mm of water.

Since the change of density of water is negligible. So the uncertainty is surface static pressure measurement.

$$\sigma_P = \left[\left(\frac{\delta_P}{\delta_{P_a}} \cdot \sigma_{P_a} \right)^2 + \left(\frac{\delta_P}{\delta_{h_w}} \cdot \sigma_{h_w} \right)^2 \right]^{1/2} \quad (8)$$

Now

$$\frac{\delta_P}{\delta_{P_a}} = 1$$

$$\frac{\delta_P}{\delta_{h_w}} = -\gamma_w \times 1/1000$$

$$\sigma_p = [\sigma_{pa}^2 + \gamma_w^2 (1/100)^2 \cdot \sigma_{hw}^2]^{1/2} \quad (9)$$

$$\frac{\sigma_p}{P} = \frac{[\sigma_{pa}^2 + \gamma_w^2 (1/1000)^2 \cdot \sigma_{hw}^2]^{1/2}}{P_a - hw \gamma_w \times 1/1000}$$

But for a short interval $\sigma_{pa} = 0$

$$\text{Hence } \frac{\sigma_p}{P} = \frac{\gamma_w (1/1000) \sigma_{hw}}{P_a - hw \gamma_w \times 1/1000}$$

Now $P = 101325 \text{ N/m}^2$

$\gamma_w = 1000 \text{ Kg/m}^3$

$hw = 6.62 \text{ mm} \pm 0.61 \text{ mm of H}_2\text{O}$

$\sigma_p / P = 4.856 \times 10^{-5}$

i.e. 0.00485%

Uncertainty in Mean velocity Measurement :

When air was flowing with a velocity of U cm/sec and pitot static tube was placed parallel to the flow, the velocity was found from the dynamic head h_u cm of water recorded by the inclined manometer from the relation.

$$u = \sqrt{2gh_u \gamma_w / \gamma_a} \quad (10)$$

where γ_w and γ_a are the specific weights of water and air respectively. If the sensing point of the pitot static tube had a misalignment of θ from the direction of flow due to adjustment error then the measured velocity would be

$$u = \sqrt{(2ghu \gamma_w / \gamma_a)} \sec\theta \quad (11)$$

using $P = \gamma_a RT$, where P, R and T are pressure, gas constant and absolute temperature of air respectively, then velocity u becomes

$$\begin{aligned} u &= \sqrt{(2ghu \gamma_w \times RT/P)} \sec \theta \\ &= \sqrt{(2gR\gamma_w)} \times \sqrt{(huT/P)} \sec \theta \\ &= C\sqrt{(hu T/P)} \sec \theta \end{aligned} \quad (12)$$

Here, $u = f (T, P, hu, \theta)$

So the uncertainty in velocity measurement can be expressed as

$$\sigma_u = \left(\frac{\delta u}{\delta P} \cdot \sigma_P \right)^2 + \left(\frac{\delta u}{\delta T} \cdot \sigma_T \right)^2 + \left(\frac{\delta u}{\delta hu} \cdot \sigma_{hu} \right)^2 + \left(\frac{\delta u}{\delta \theta} \cdot \sigma_\theta \right)^2 \quad (13)$$

Where σ_p , σ_T , σ_{hu} and $\sigma\theta$ are uncertainties associated with pressure, temperature, digital manometer regarding and alignment of the probe with the flow direction.

To get the uncertainties involved in the different variables the respective partial derivatives are now found out. Again writing equation (12) in the form

$$u = C \sqrt{(hu T/P)} \text{Sec } \theta$$

The partial derivatives of U are found to be

$$\frac{\delta u}{\delta P} = C \sqrt{hu} \cdot T \cdot \text{Sec } \theta (-1/2P^{-3/2}) = -\frac{C}{2} \frac{\sqrt{huT}}{P^3} \cdot \text{Sec } \theta \quad (14)$$

$$\frac{\delta u}{\delta T} = C \frac{\sqrt{hu}}{P} \cdot \text{Sec } \theta \cdot \frac{1}{2} T^{-1/2} = C/2 \frac{\sqrt{hu}}{PT} \cdot \text{Sec } \theta \quad (15)$$

$$\frac{\delta u}{\delta h} = C \sqrt{\frac{T}{P}} \cdot \text{Sec } \theta \cdot \frac{1}{2} hu^{-1/2} \quad (16)$$

$$\text{and } \frac{\delta u}{\delta \theta} = C \sqrt{\frac{huT}{P}} \cdot \text{Sec } \theta \cdot \tan \theta \quad (17)$$

Putting these equations to equation (13) We get

$$\sigma_u = \left[\left(-\frac{C}{2} \sqrt{\frac{huT}{P^3}} \cdot \text{Sec } \theta \cdot \sigma_P \right)^2 + \left(\frac{C}{2} \text{Sec } \theta \frac{\sqrt{hu}}{PT} \cdot \sigma_T \right)^2 + \left(\frac{C}{2} \sqrt{\frac{T}{Ph}} \cdot \text{Sec } \theta \cdot \sigma_h \right)^2 + \left(C \sqrt{\frac{hu}{P}} \text{Sec } \theta \cdot \tan \theta \cdot \sigma_\theta \right)^2 \right]^{1/2}$$

$$\begin{aligned}
&= \left[\frac{C^2}{4} \cdot \frac{huT}{P^3} (\sec\theta)^2 \sigma_p^2 + \frac{C^2}{4} \cdot \frac{hu}{TP} (\sec\theta)^2 \cdot \sigma T^2 + \frac{C^2}{4} \cdot \frac{T}{P_{hu}} \sec^2\theta \sigma_{hu}^2 + \right. \\
&\quad \left. C^2 \frac{T_{hu}}{P} \cdot \sec^2\theta \cdot \tan^2\theta \cdot \delta\theta^2 \right]^{1/2} \\
&= \frac{C}{2} \cos\theta \left[\left(\frac{huT}{P^3} \right) \sigma_p^2 + \left(\frac{hu}{TP} \right) \sigma_T^2 + \left(\frac{T}{P_{hu}} \right) \sigma_{hu}^2 + 4 \left(\frac{huT}{P} \sigma\theta^2 \cdot \tan^2\theta \right) \right]^{1/2} \quad (18)
\end{aligned}$$

Now dividing equation (18) by equation (12) the uncertainty in velocity measurement takes the form.

$$\frac{\sigma_u}{u} = \frac{1}{2} \left[\frac{\sigma_p^2}{P^2} + \frac{\sigma T^2}{T^2} + \frac{\sigma_{hu}^2}{hu^2} + 4\sigma\theta^2 \cdot \tan^2\theta \right]^{1/2}$$

The direction is taken for objective uncertainties. There is also subjective uncertainties which is considered 5%, So the final uncertainties becomes

$$\frac{\sigma_u}{u} = 1/2 \left[\frac{\sigma_p^2}{P^2} + \frac{\sigma T^2}{T^2} + \frac{\sigma_{hu}^2}{hu^2} + 4\sigma\theta^2 \cdot \tan^2\theta + \delta^2 \right]^{1/2}$$

Now during an experimental run, the following conditions were observed.

$$\begin{aligned}
P &= 76.2 \text{ cm} \pm 0.10 \text{ cm H}_2\text{O} \\
T &= 82^\circ \pm 2^\circ\text{F} \\
hu &= 2.61 \text{ cm H}_2\text{O} \pm 0.0254 \text{ cm of H}_2\text{O} \\
\theta &= 0^\circ \pm 2^\circ
\end{aligned}$$

The corresponding uncertainty in velocity measurement becomes

$$\sigma_u/u = 2.82\%$$

FIGURES

- | | |
|-----------------------|----------------------|
| 1. Settling chamber | 2. Converging mouth |
| 3. Honey comb section | 4. Perspex section |
| 5. Test section | 6. Wood section |
| 7. Wood section | 8. Diverging section |
| 9. Fan 1 | 10. Fan 2 |
| 11. Butterfly valve | 12. Silencer |

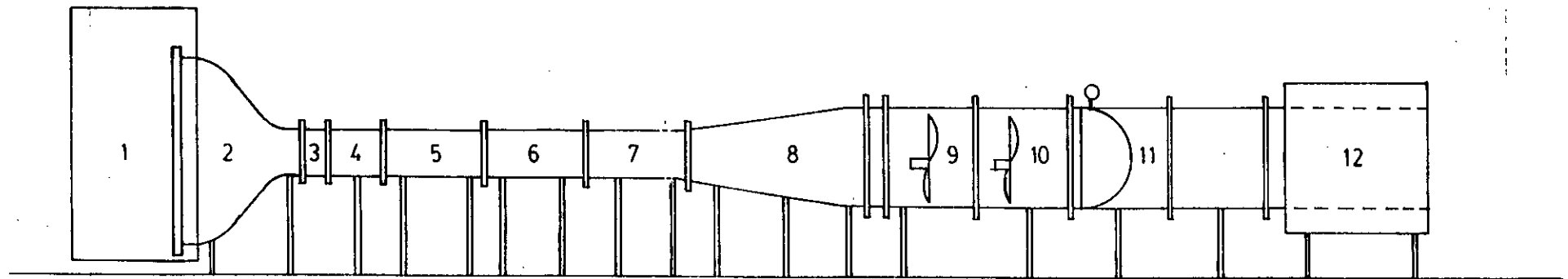


Fig. 3.1 : Schematic diagram of the wind tunnel.

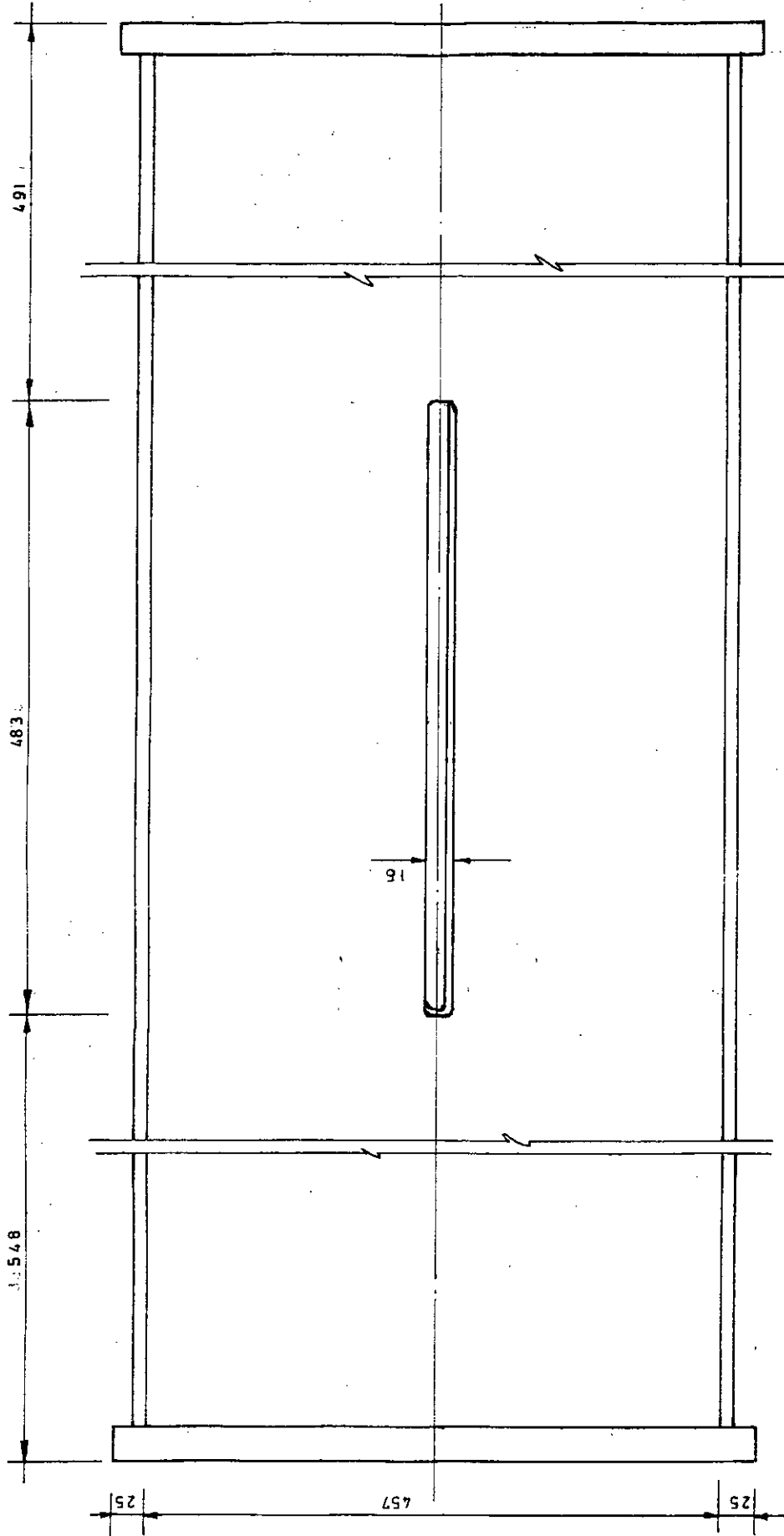


FIG. 3.2 : Perspex vertical side wall of the test section (all dimensions are in mm)

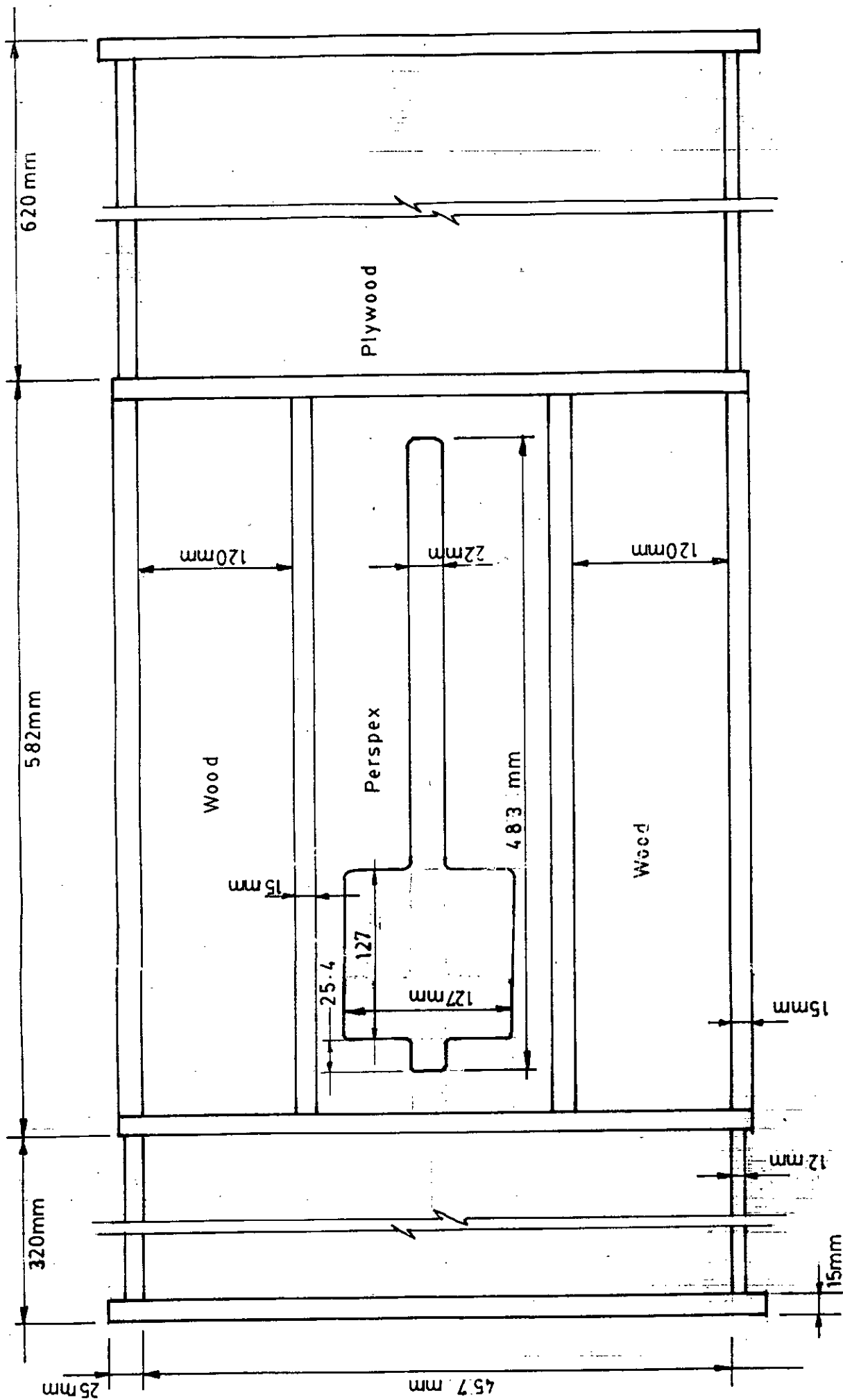


Fig. 3.3 : Perspex and wooden vertical wall side.

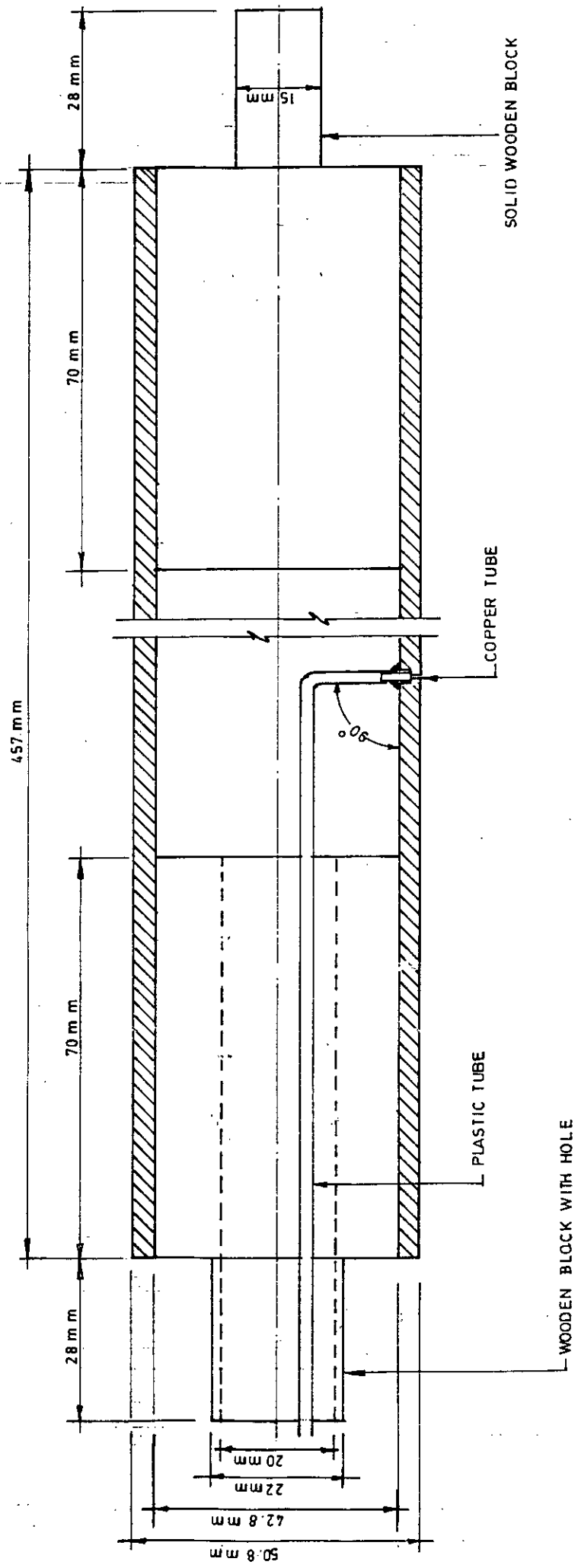


FIG: 3.4: Sectional view of a specimen square Cylinder

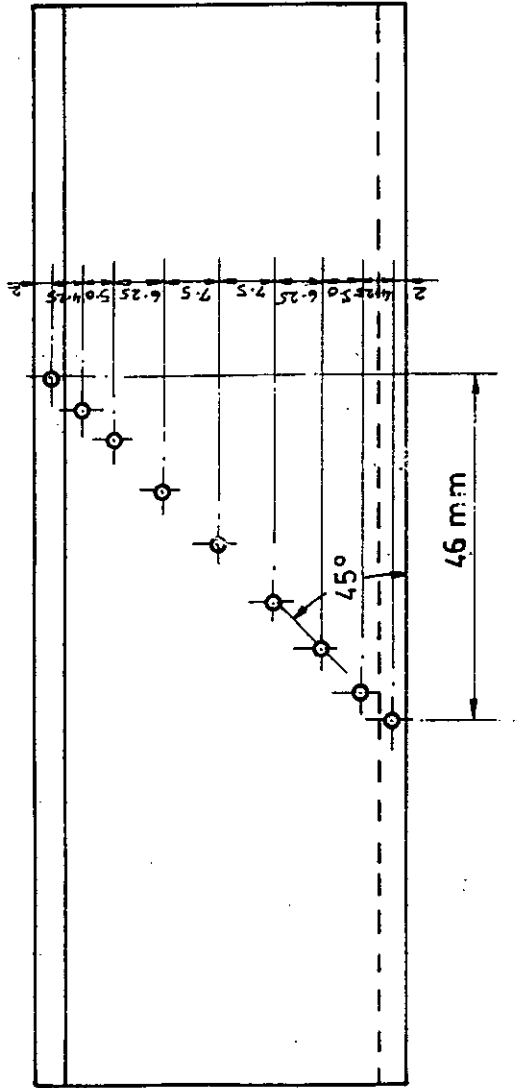


Fig. 3.5.7 The arrangement of tapping points on adjacent side

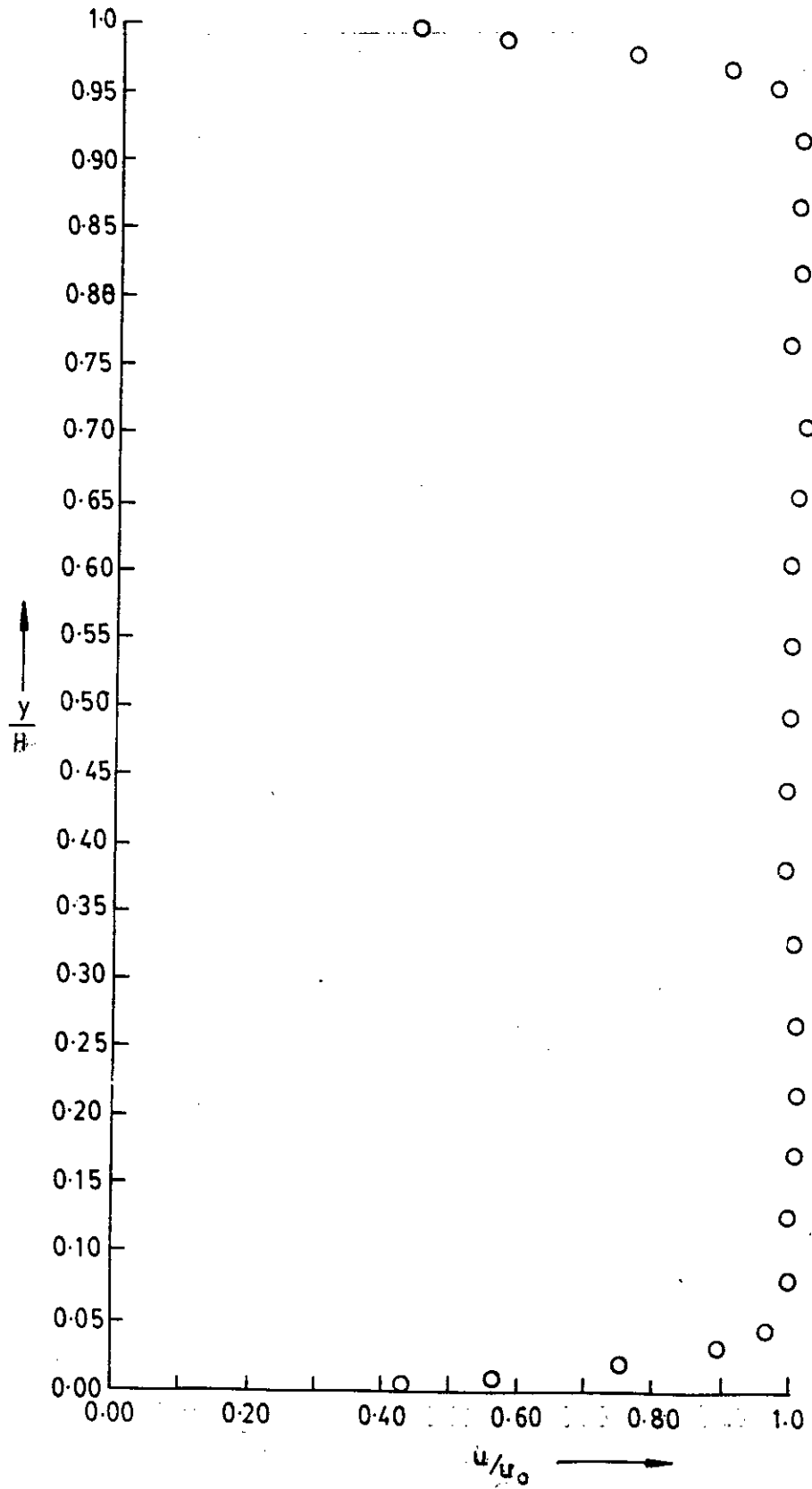
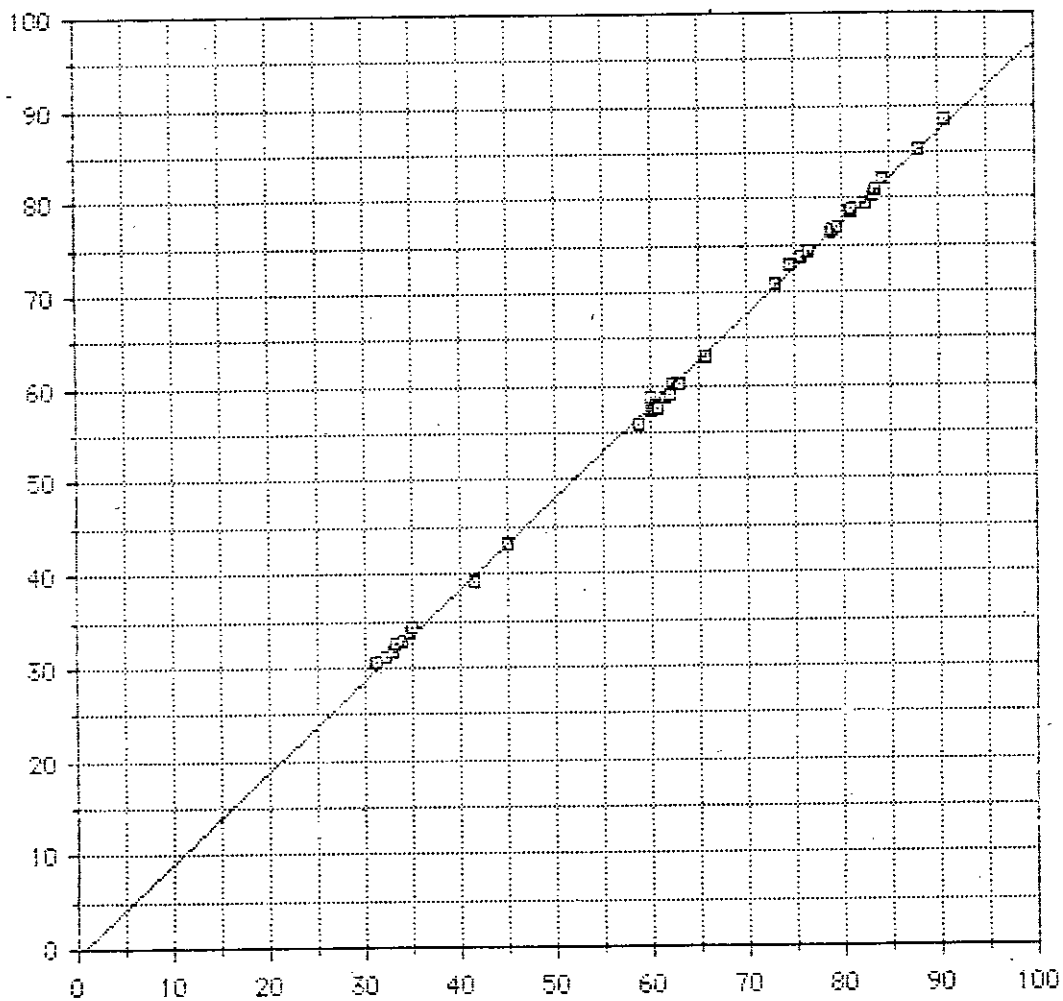


Fig. 3.6 : Velocity distribution in upstream side of the test section.

micro reading (mm water)



trans-reading (mm water)

3.7 : Calibrated Micromanometer against U-type manometer.

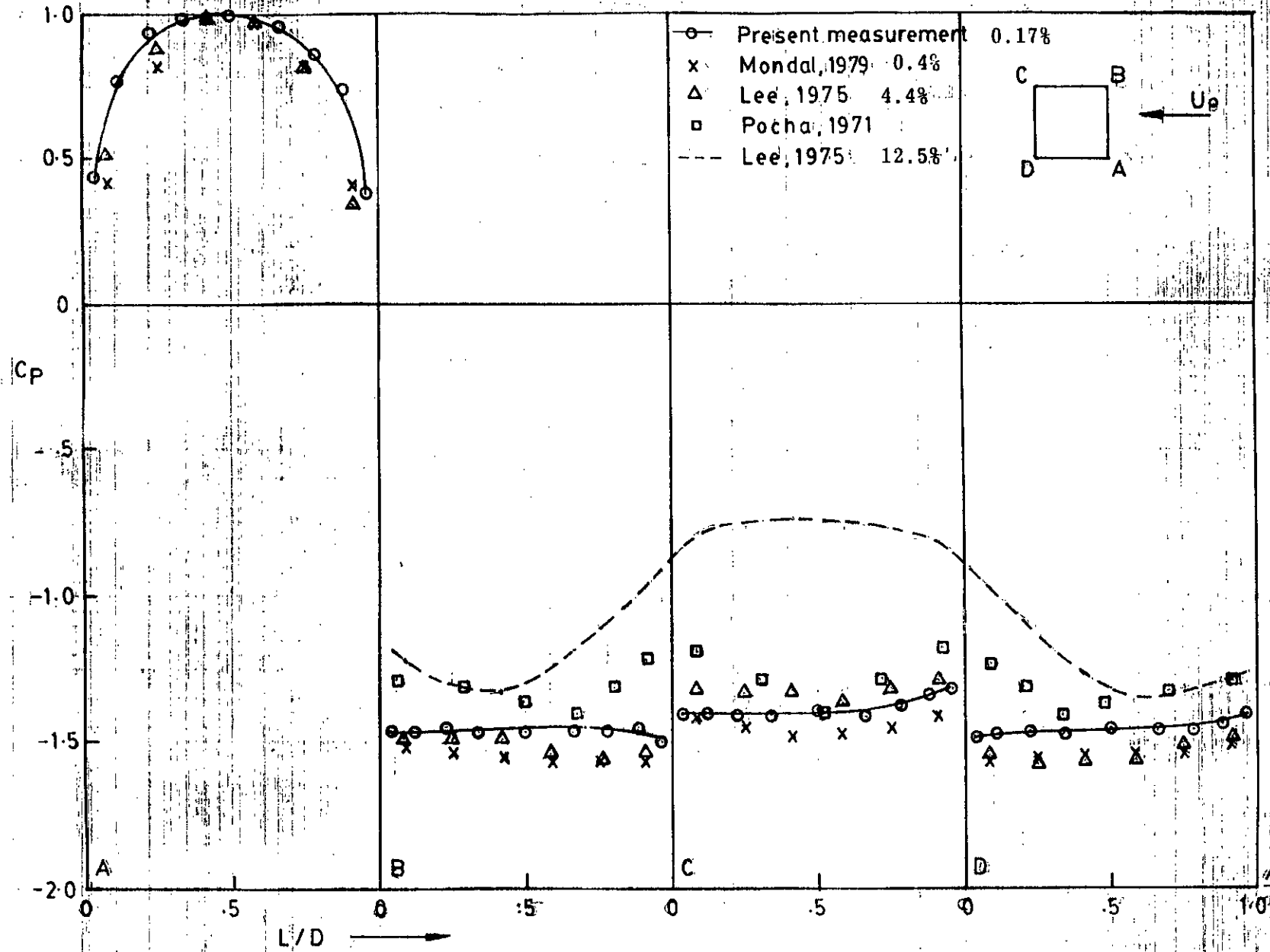


Fig. 4.1 : Comparison of C_p -distribution on a square cylinder.

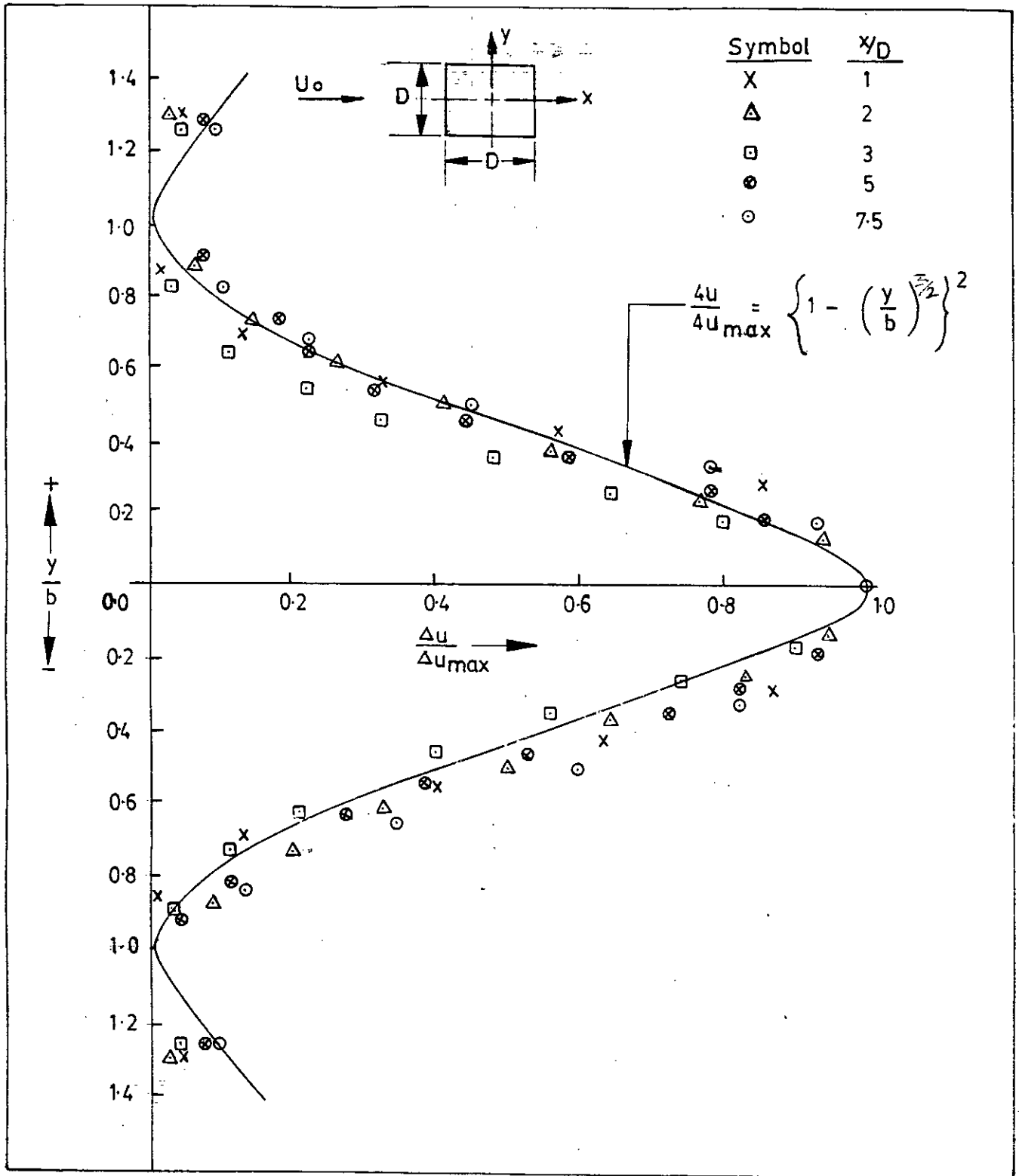


Fig. 4.2 : Velocity distribution in a two dimensional wake behind a square cylinder.

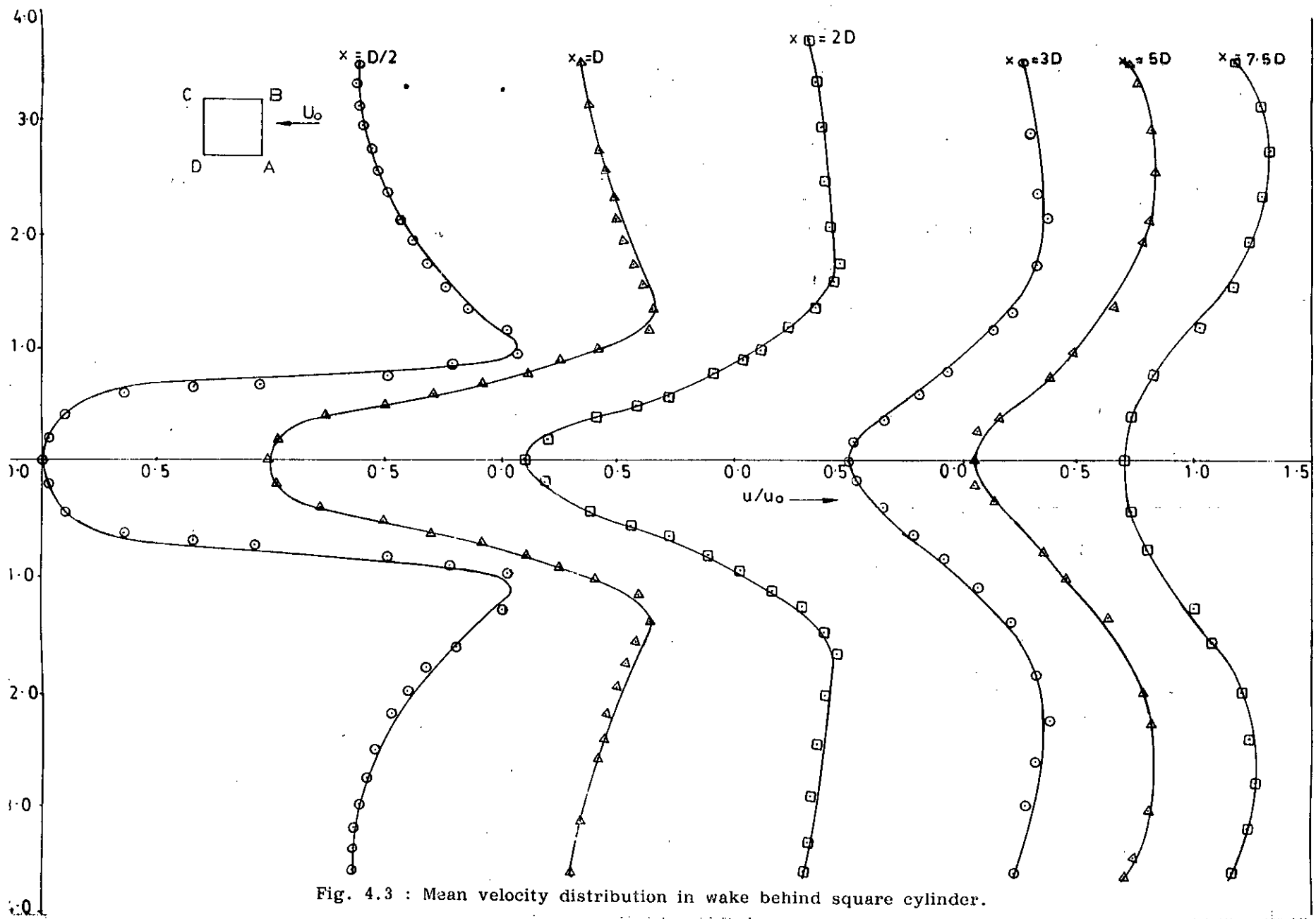


Fig. 4.3 : Mean velocity distribution in wake behind square cylinder.

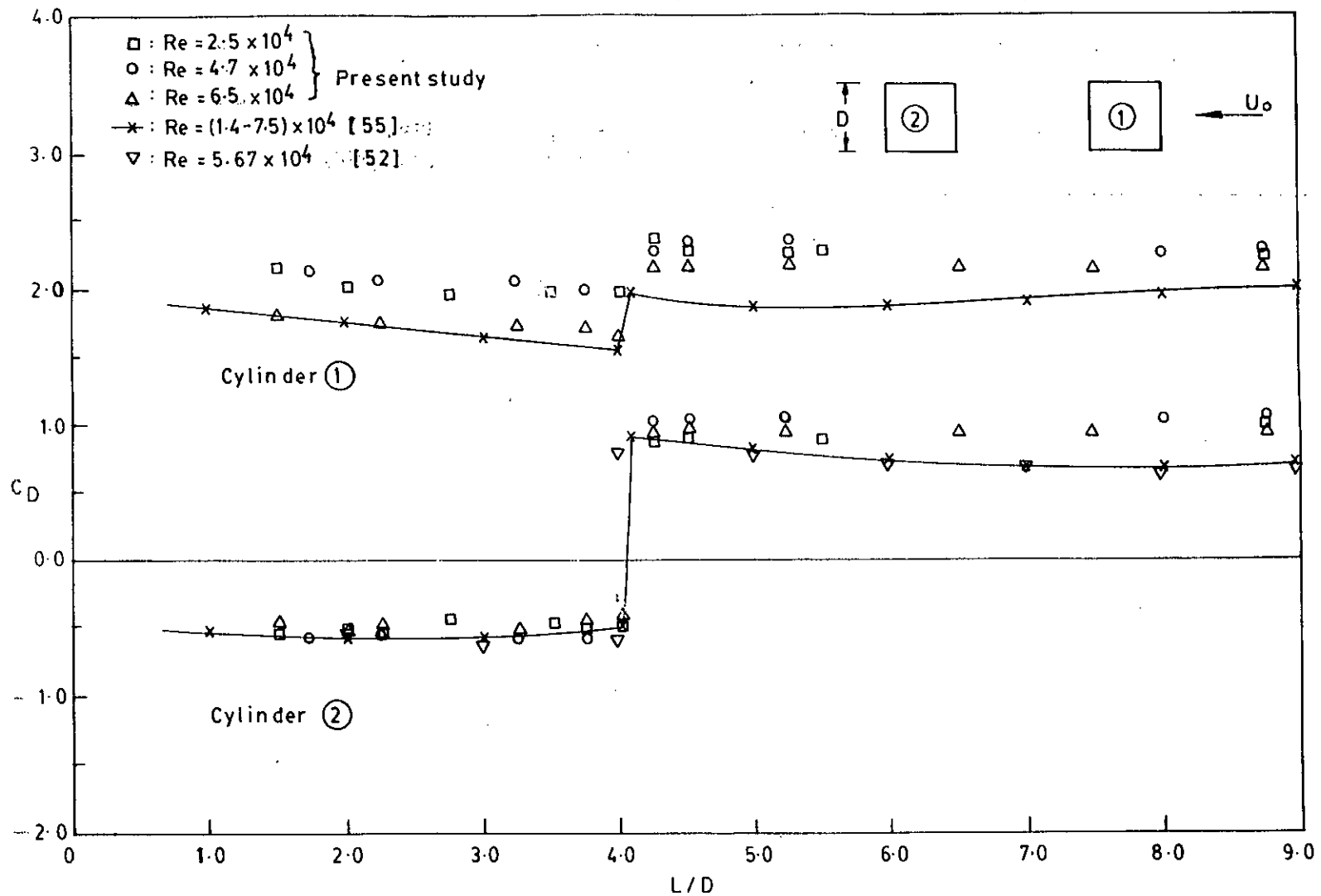


Fig. 4.4 : Comparison of drag co-efficient of two tandem square cylinders for different Reynolds number.

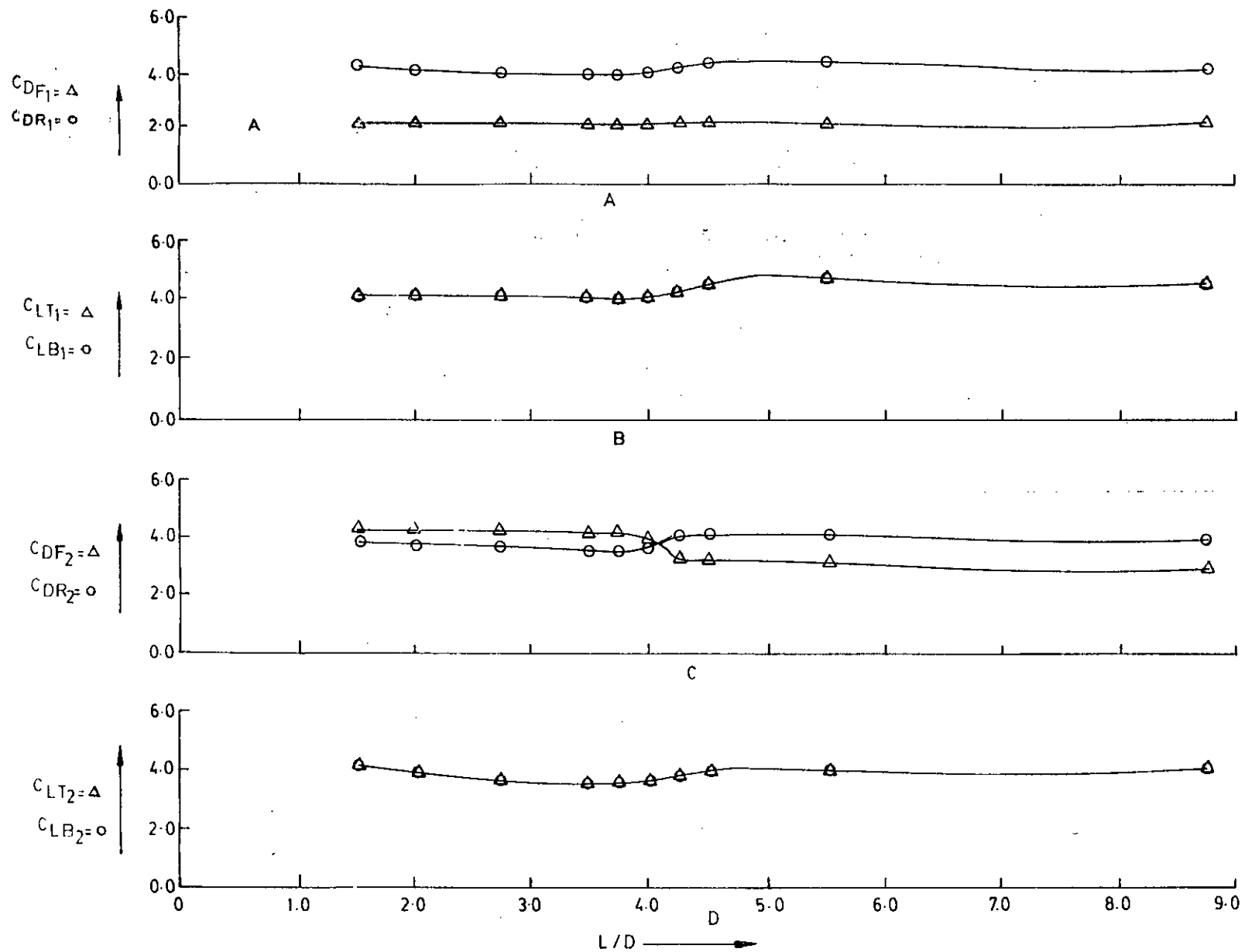


Fig. 4.5 : Variation of drag and lift forces on the surface of two tandem square cylinders due to change in inter spacing at Reynolds number of 2.5×10^4 .

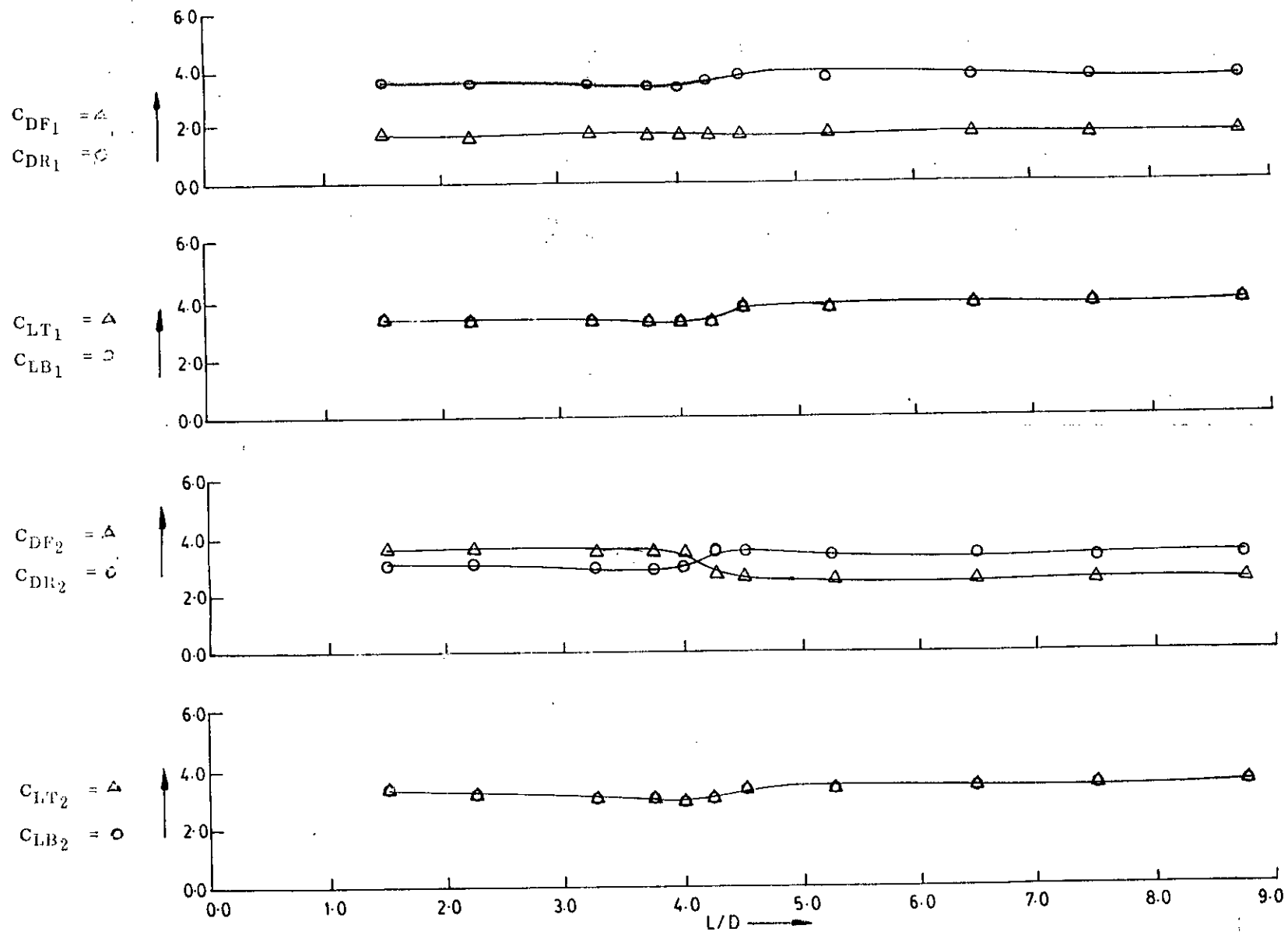


Fig. 4.6 : Variation of drag and lift forces on the surface of two tandem square cylinders due to change in inter spacing at Reynolds number of 4.7×10^4 .

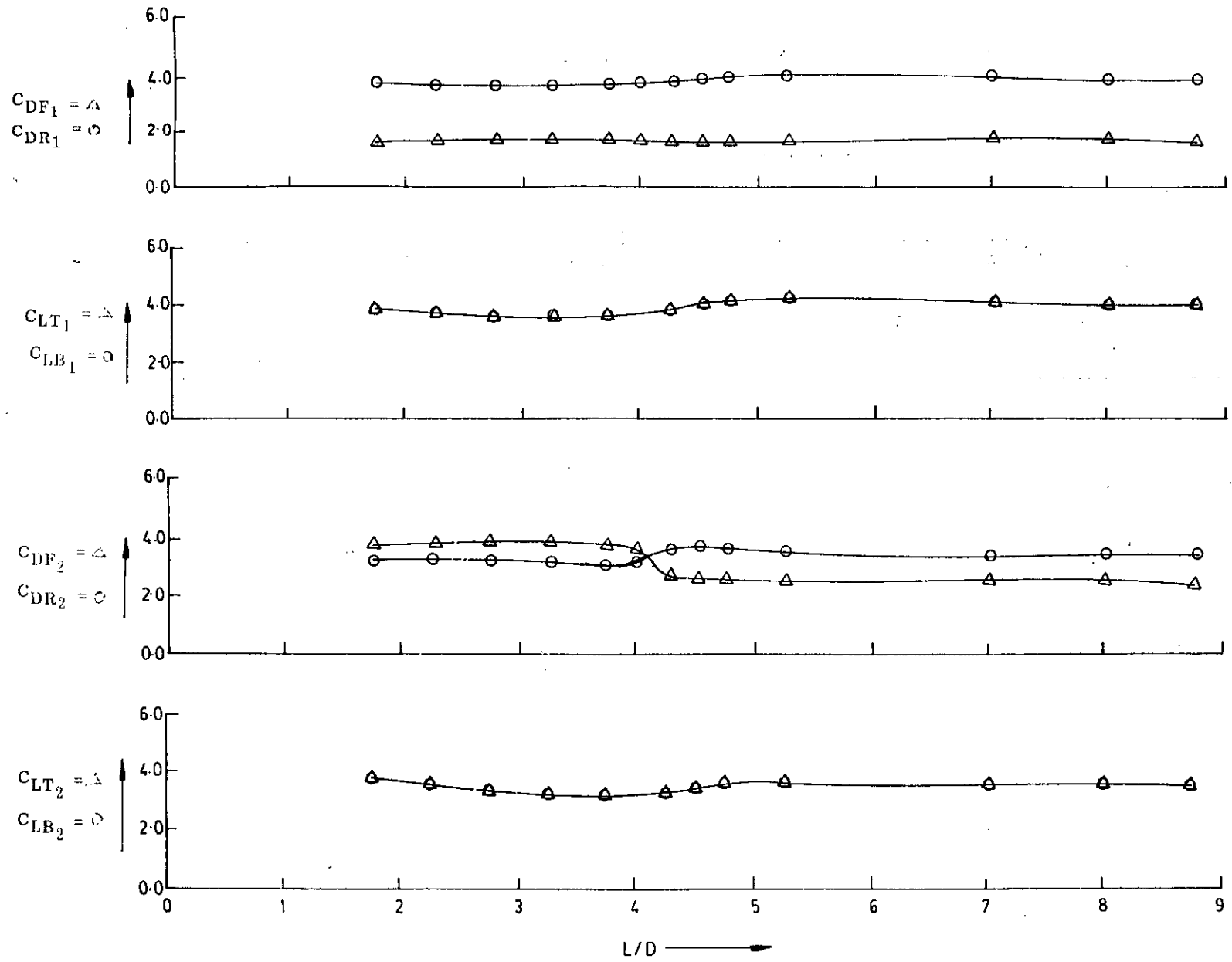


Fig. 4.7 : Variation of drag and lift forces on the surface of two tandem square cylinders due to change in inter spacing at Reynolds number of 6.5×10^4 .

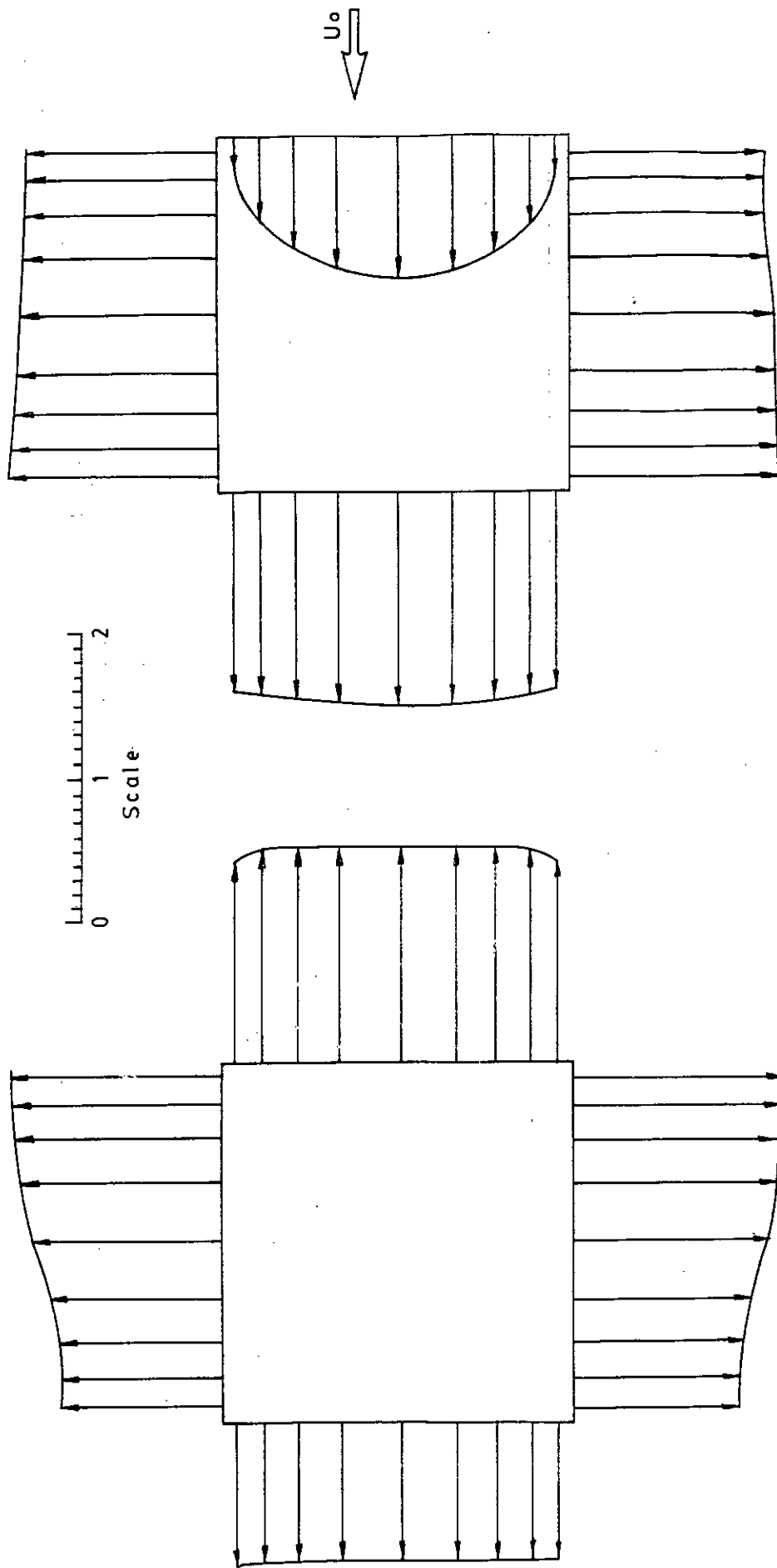


Fig. 4.8 : Mean pressure distribution around two square cylinders for $L/D = 1.5$ at Reynolds number of 2.5×10^4 .

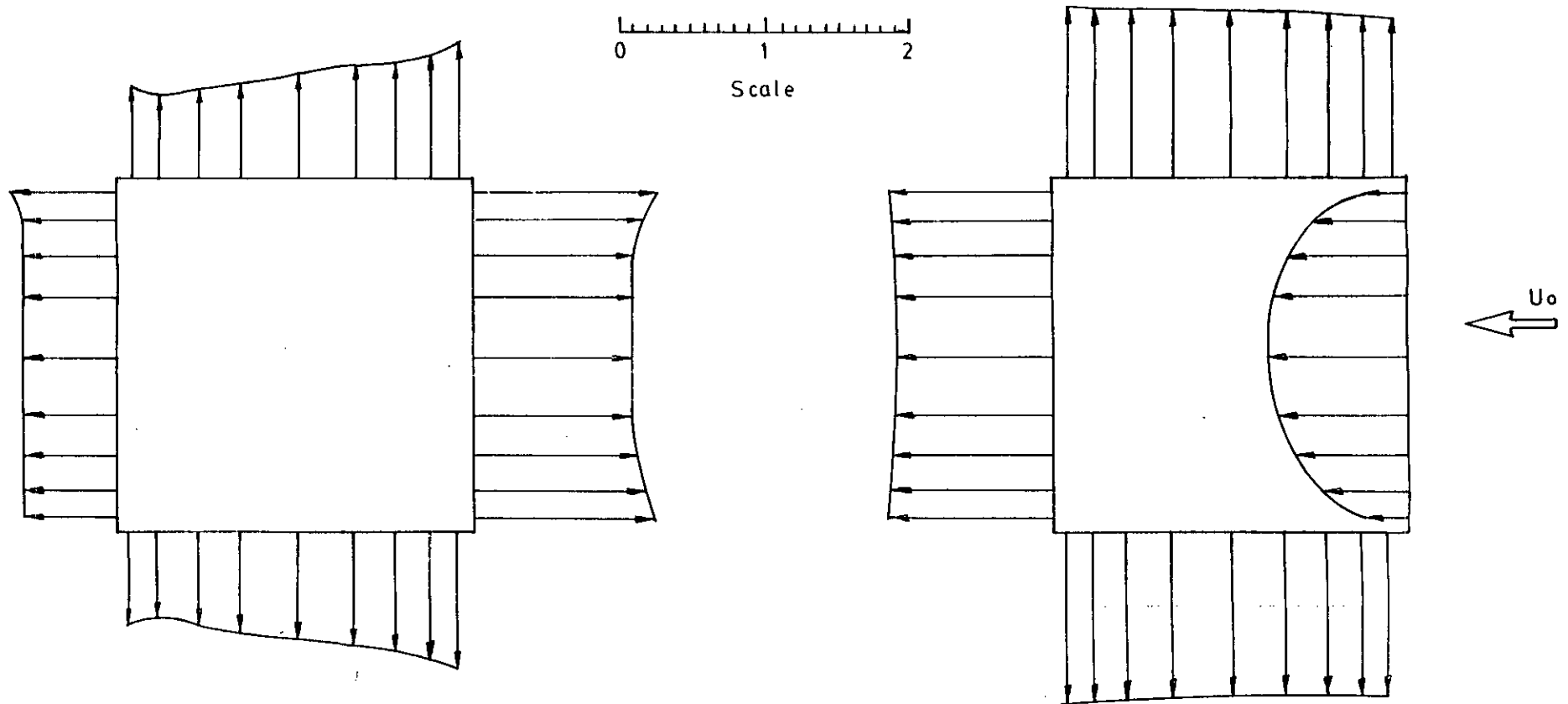


Fig. 4.9 : Mean pressure distribution around two square cylinders for $L/D = 4.0$ at Reynolds number of 2.5×10^4 .

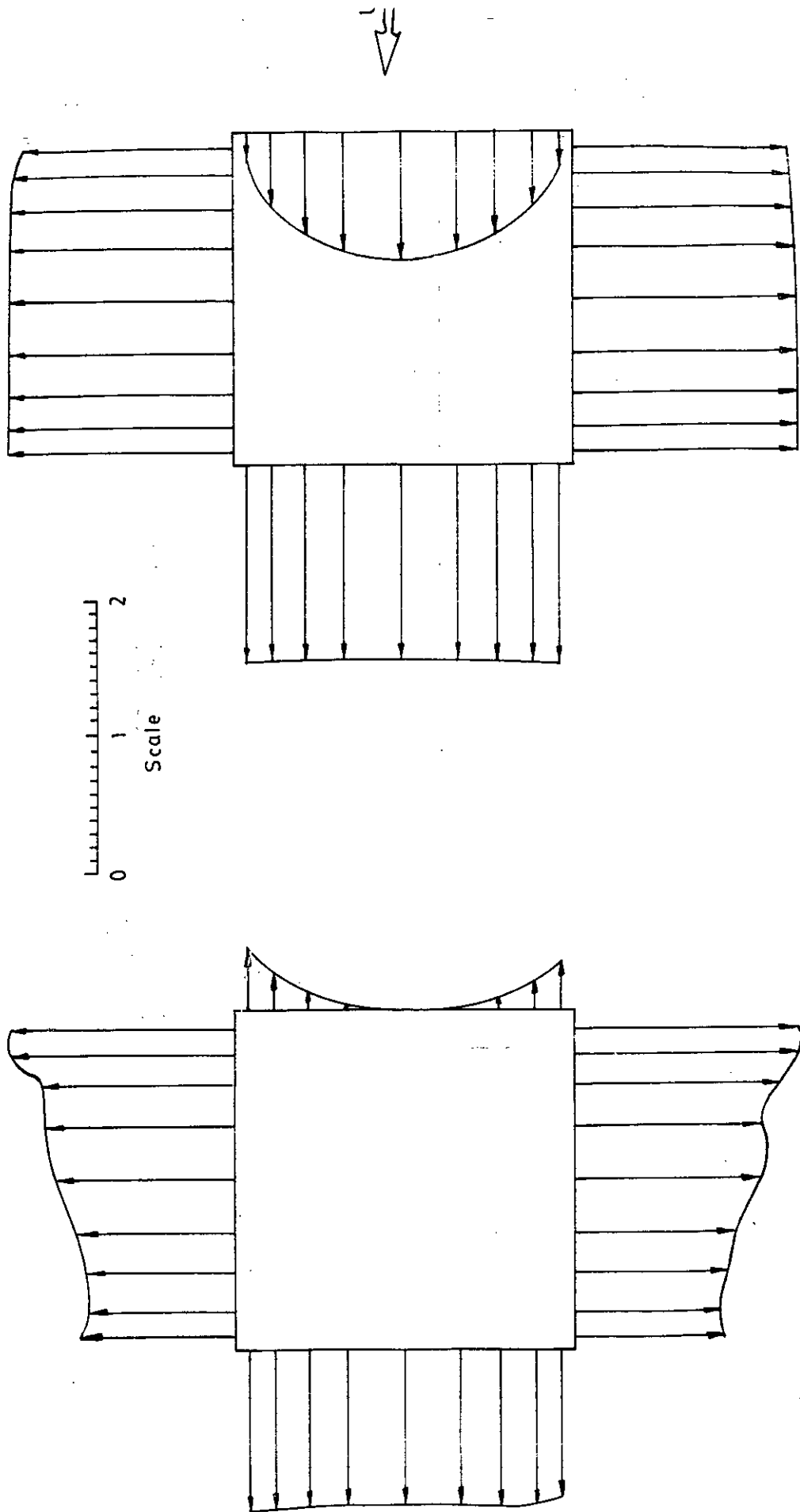


Fig. 4.10 : Mean pressure distribution around two square cylinders for L/D 8.75 at Reynolds number of 2.5×10^4 .

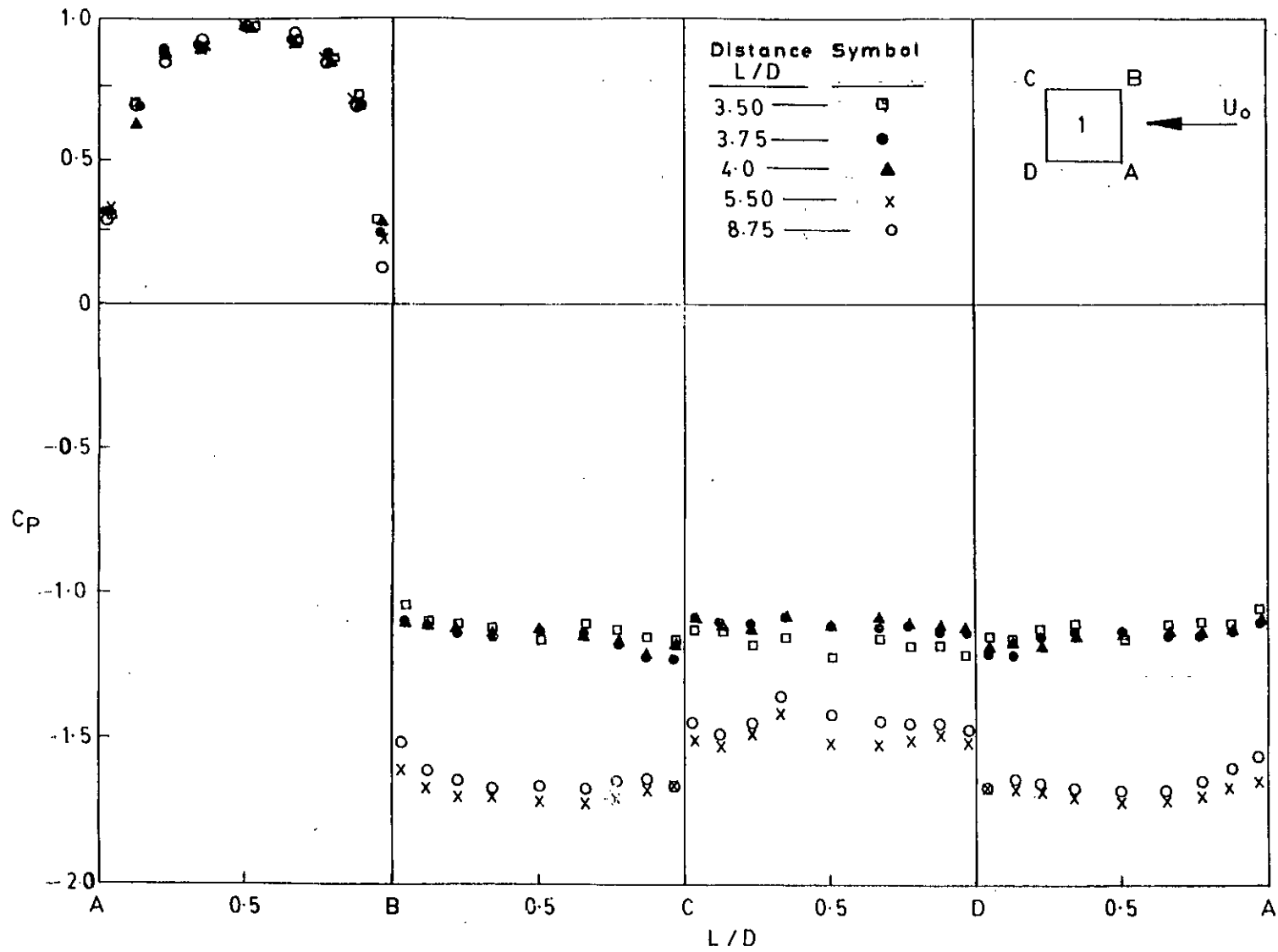


Fig. 4.11 : Effect of L/D on C_p distribution around upstream cylinder with Reynolds number of 2.5×10^4 .

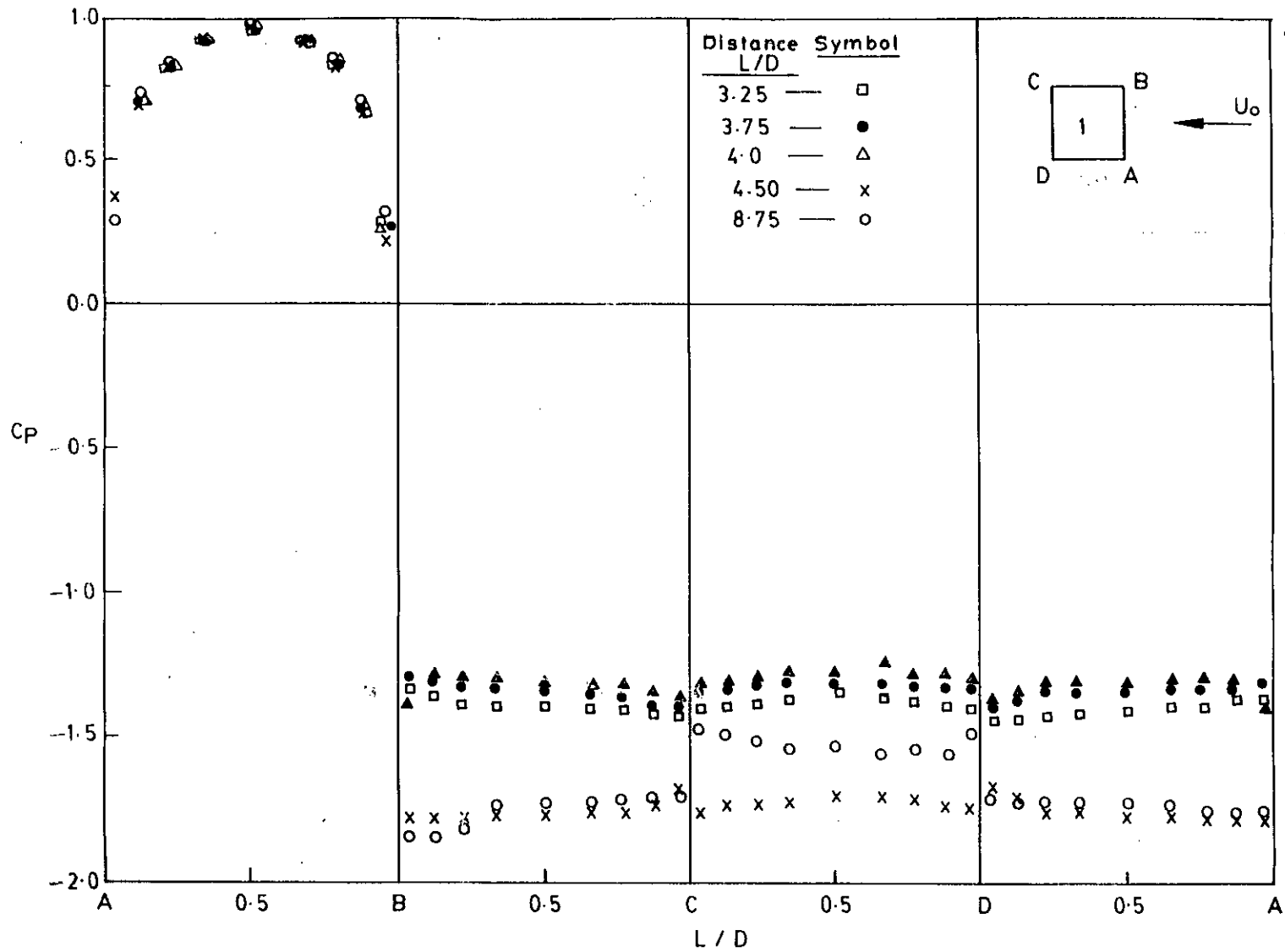


Fig. 4.12 : Effect of L/D on C_p distribution around upstream cylinder with Reynolds number of 4.7×10^4 .

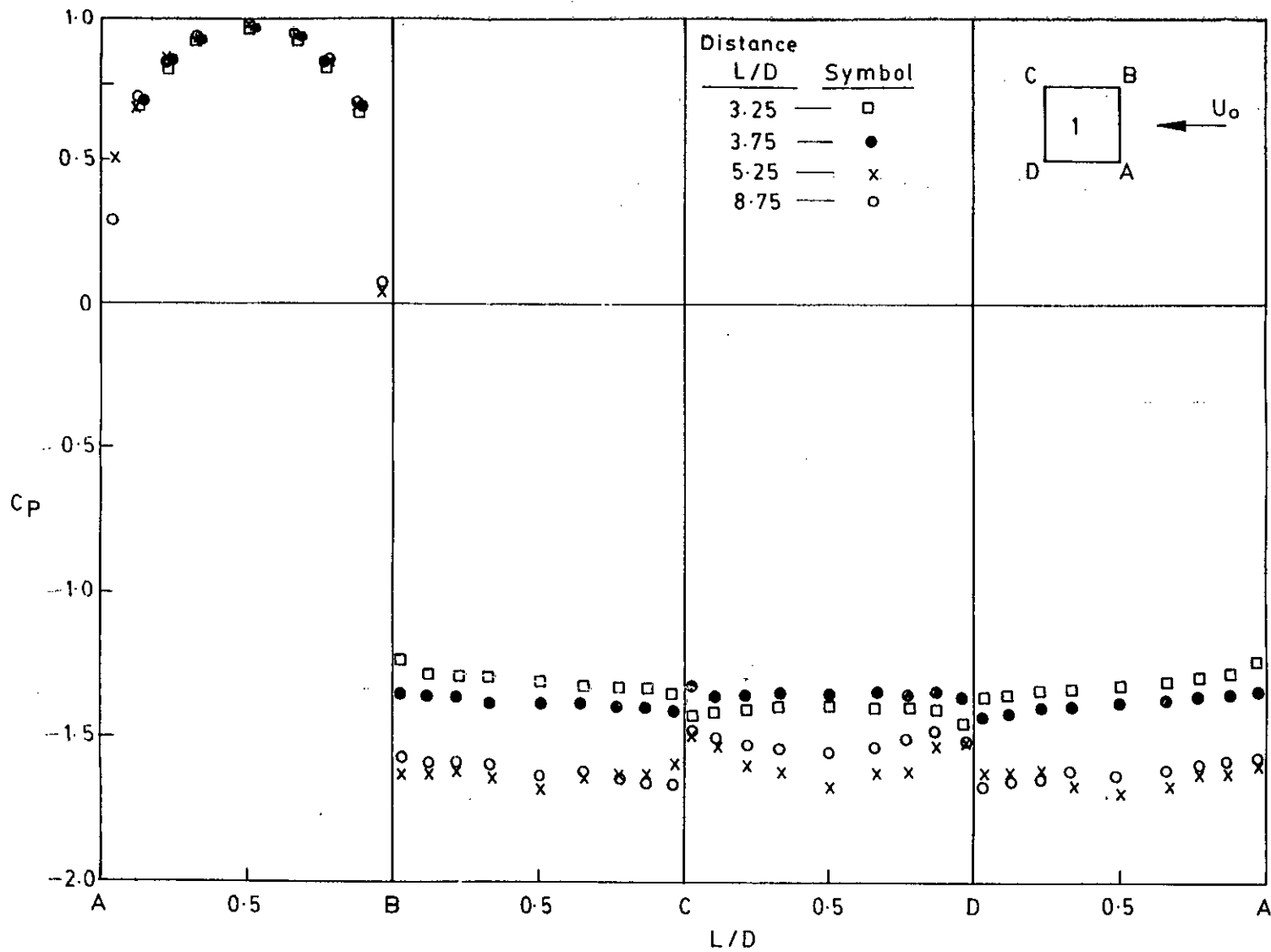


Fig. 4.13 : Effect of L/D on C_p distribution around upstream cylinder with Reynolds number of 6.5×10^4 .

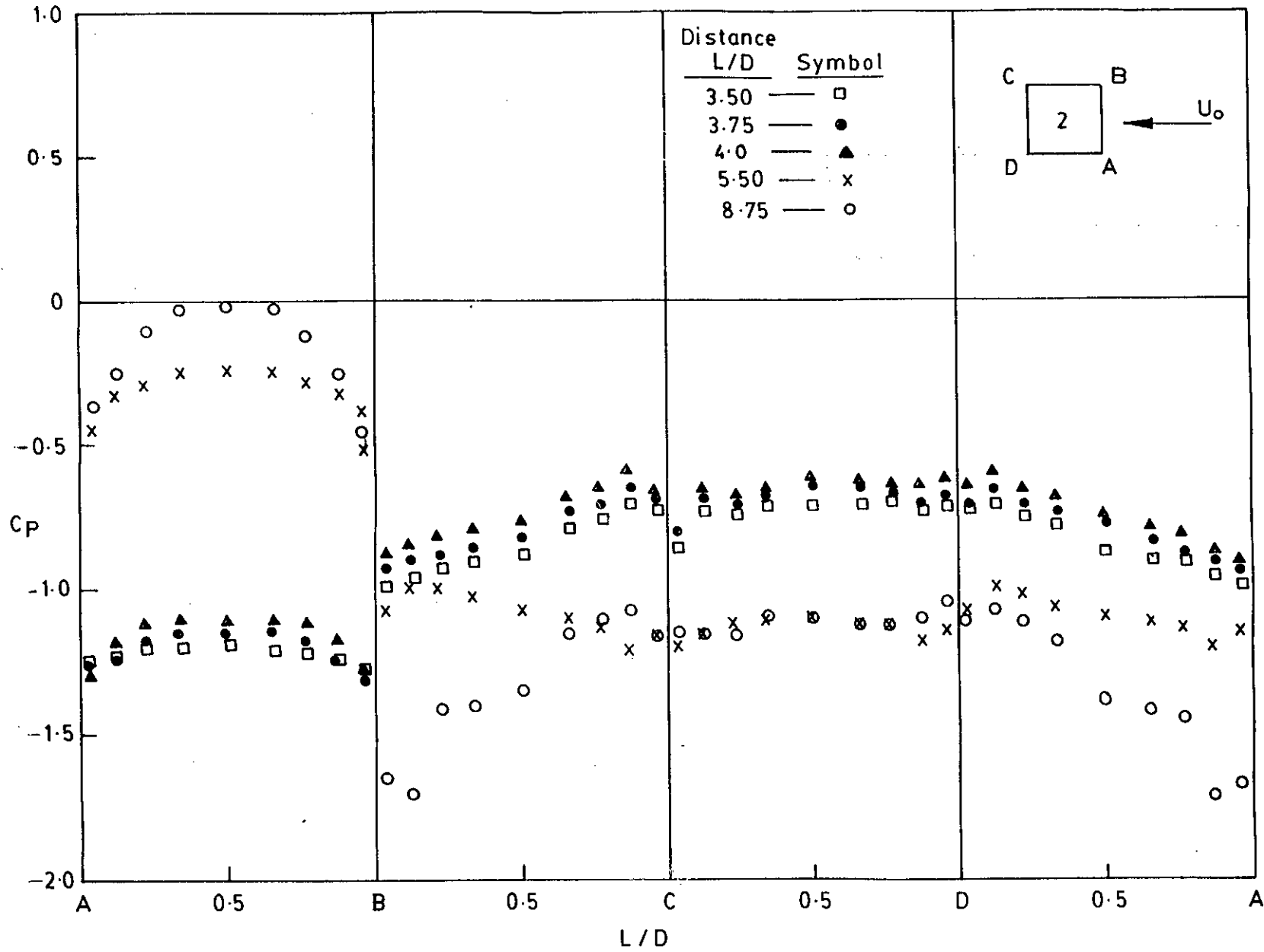


Fig. 4.14 : Effect of L/D on C_p distribution around downstream cylinder with Reynolds number of 2.5×10^4 .

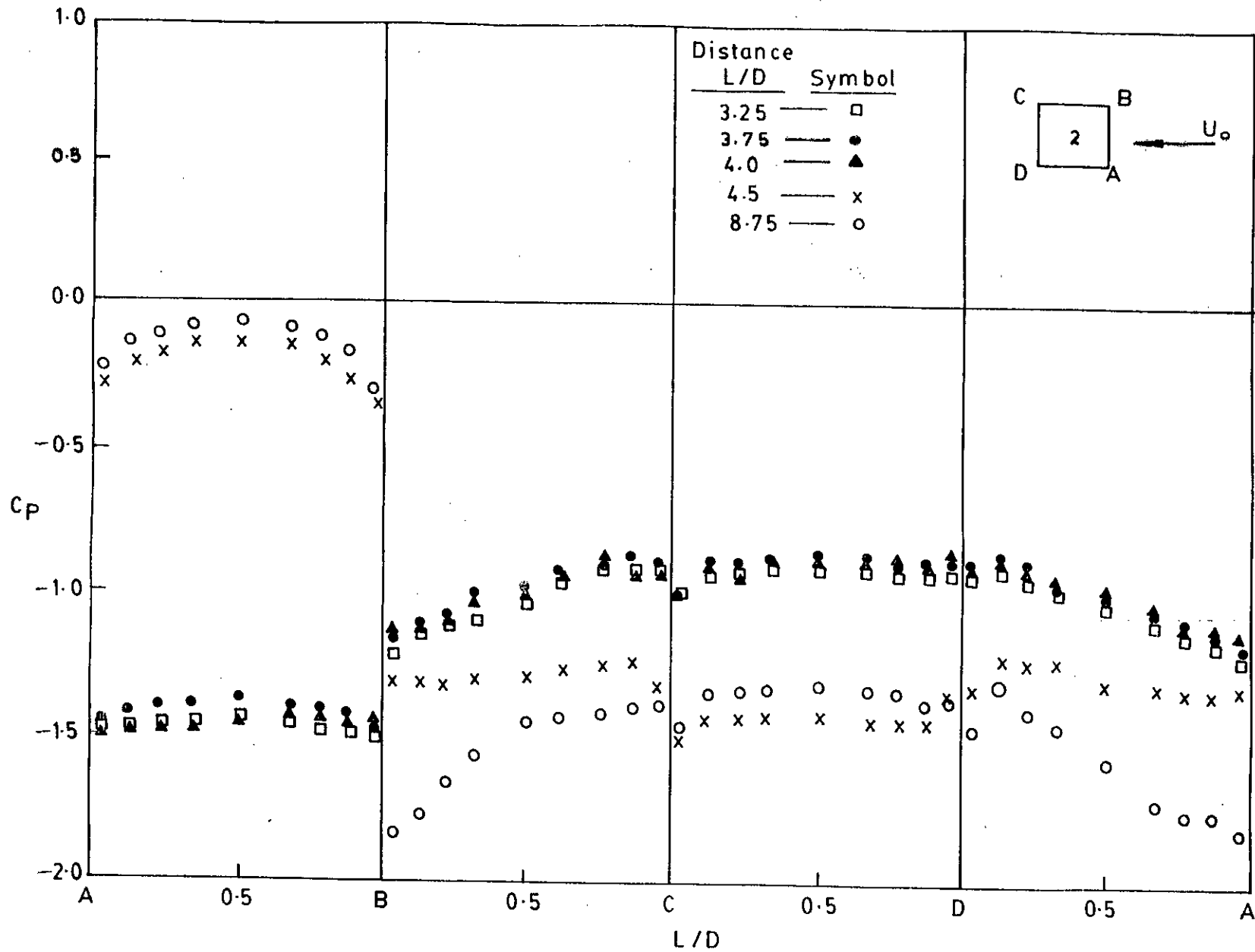


Fig. 4.15 : Effect of L/D on C_p distribution around downstream cylinder with Reynolds number of 4.7×10^4 .

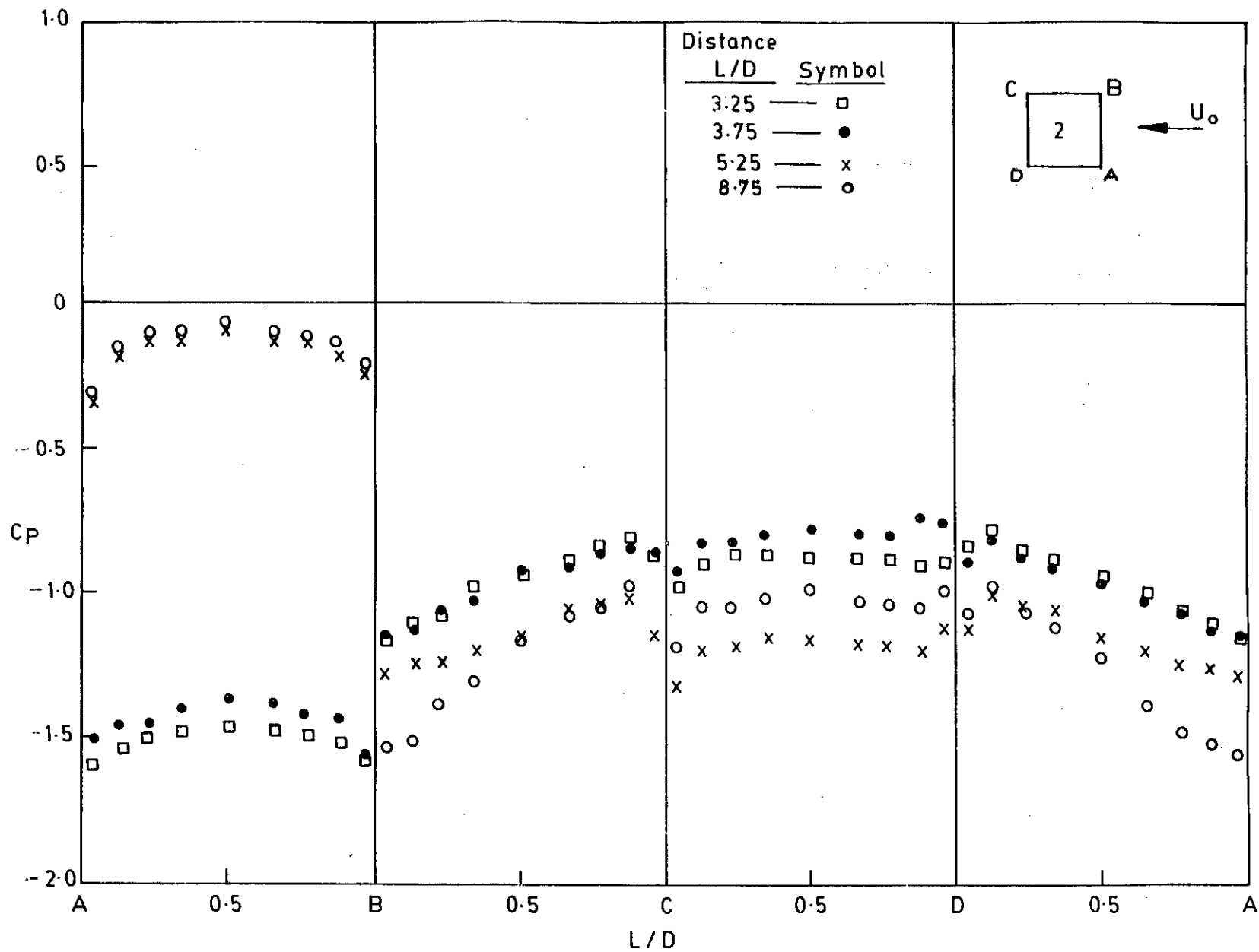


Fig. 4.16 : Effect of L/D on C_p distribution around downstream cylinder with Reynolds number of 6.5×10^4 .

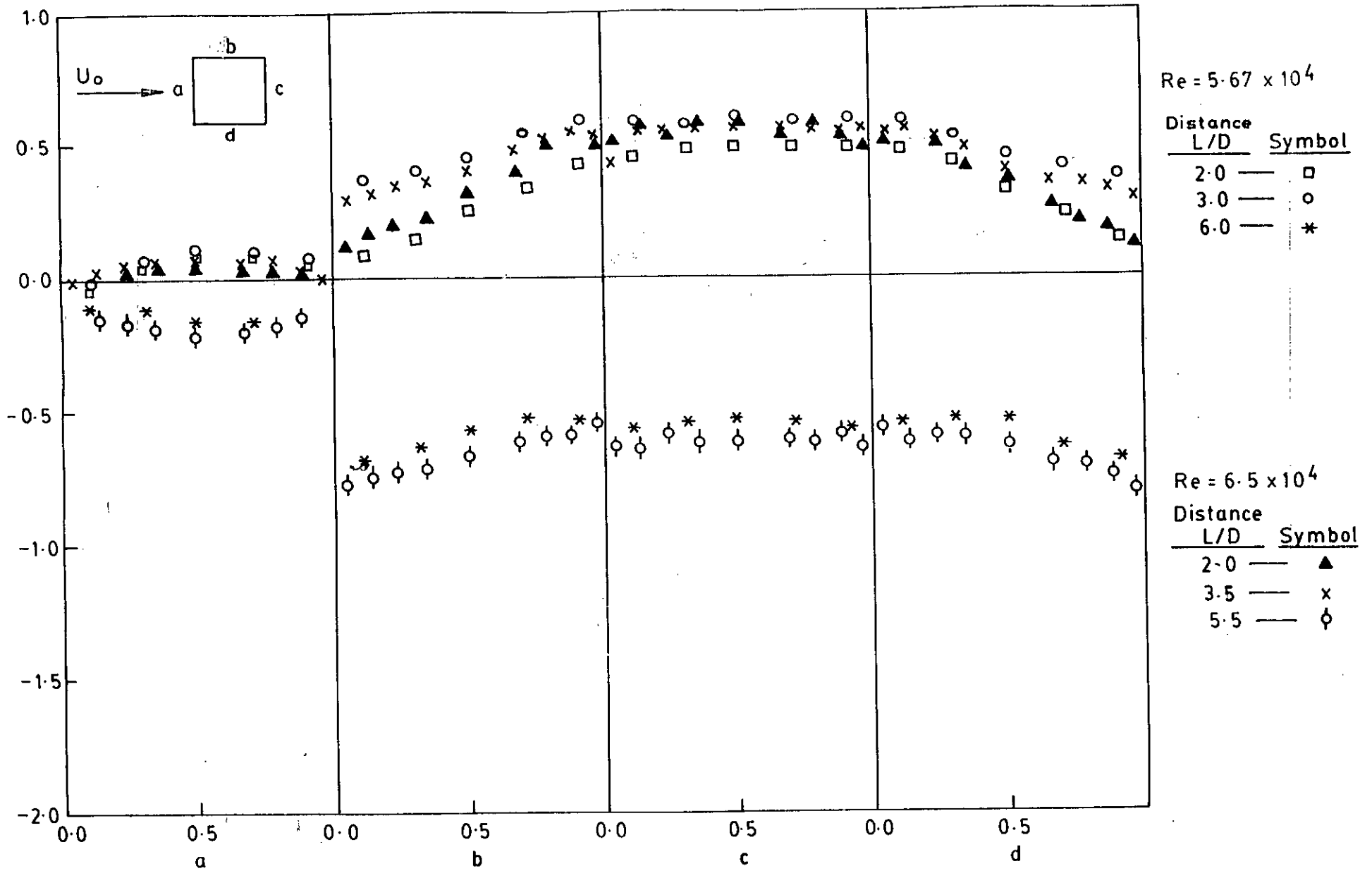


Fig. 4.16 (a) : Comparison of C_p distribution around downstream cylinder with Reynolds number 5.6×10^4 .

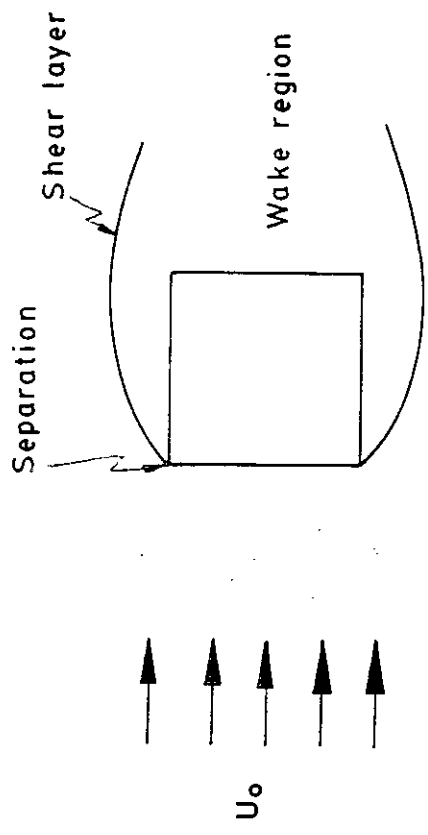


Fig. 4.16 (b): The nature of flow pattern around square prism.

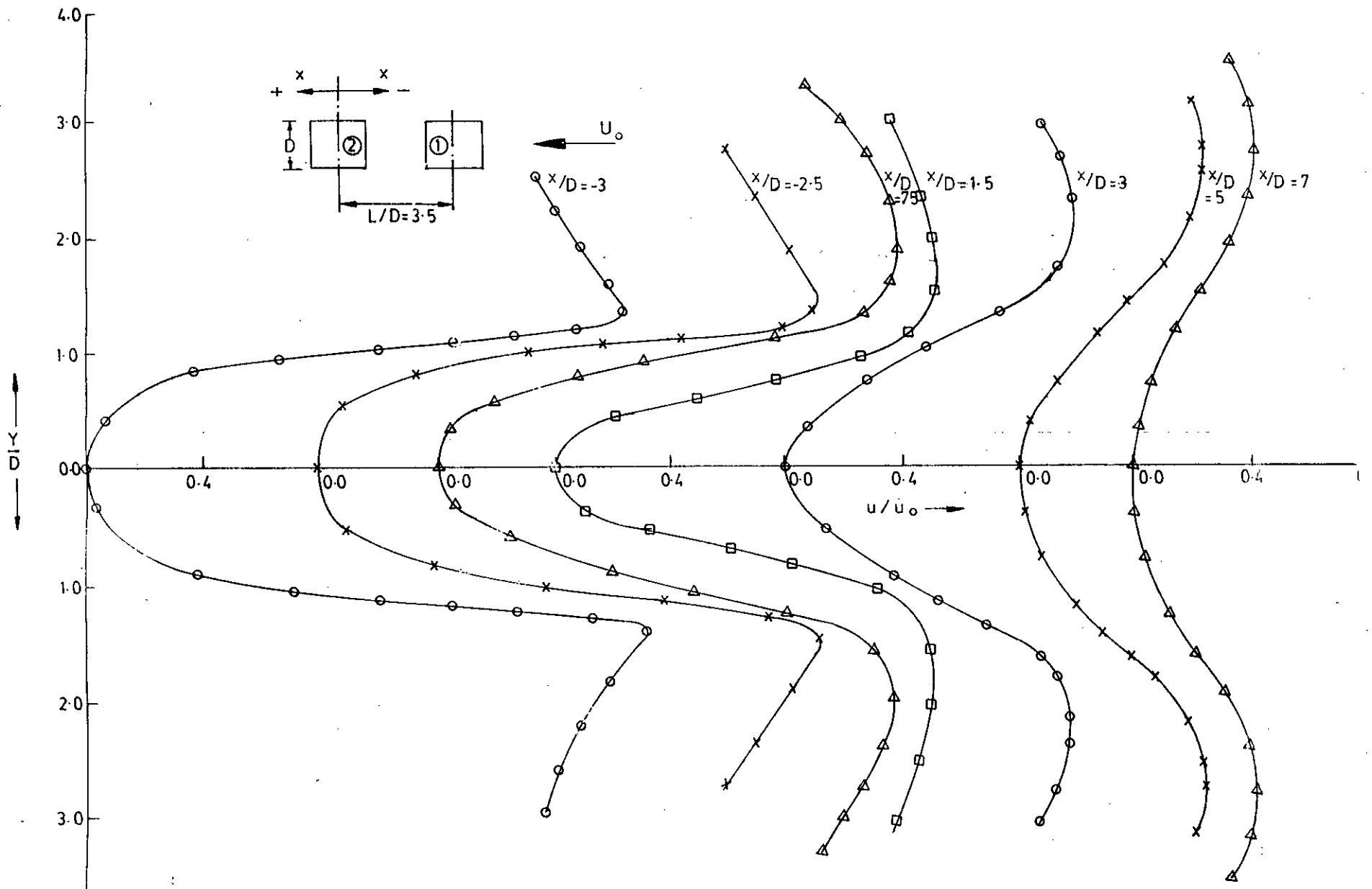


Fig. 4.17 : Mean velocity distribution in wakes behind upstream and downstream square cylinders arranged in tandem for $L/D = 3.5$

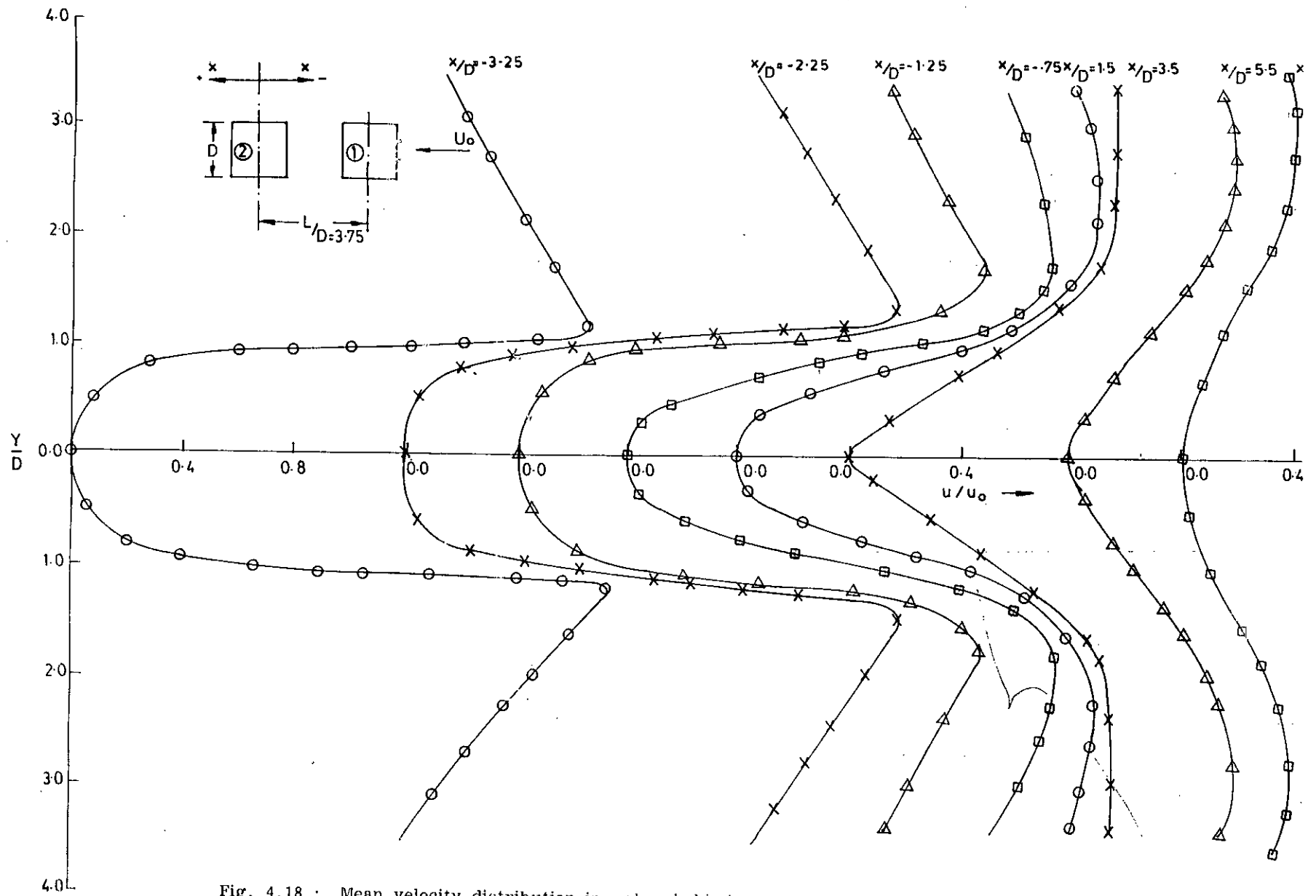


Fig. 4.18 : Mean velocity distribution in wakes behind upstream and downstream square cylinders arranged in tandem for $L/D = 3.75$

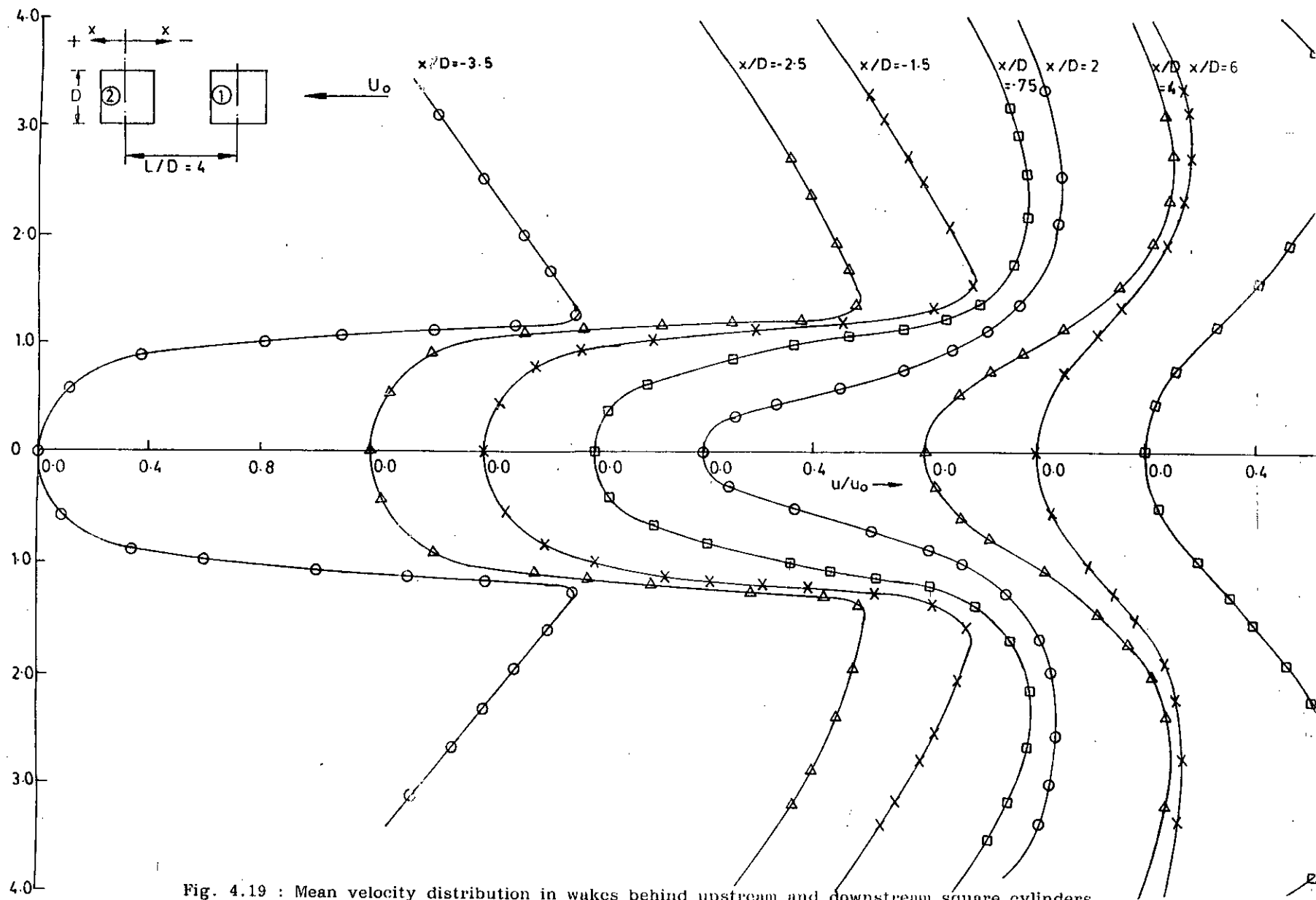


Fig. 4.19 : Mean velocity distribution in wakes behind upstream and downstream square cylinders arranged in tandem for $L/D = 4.0$

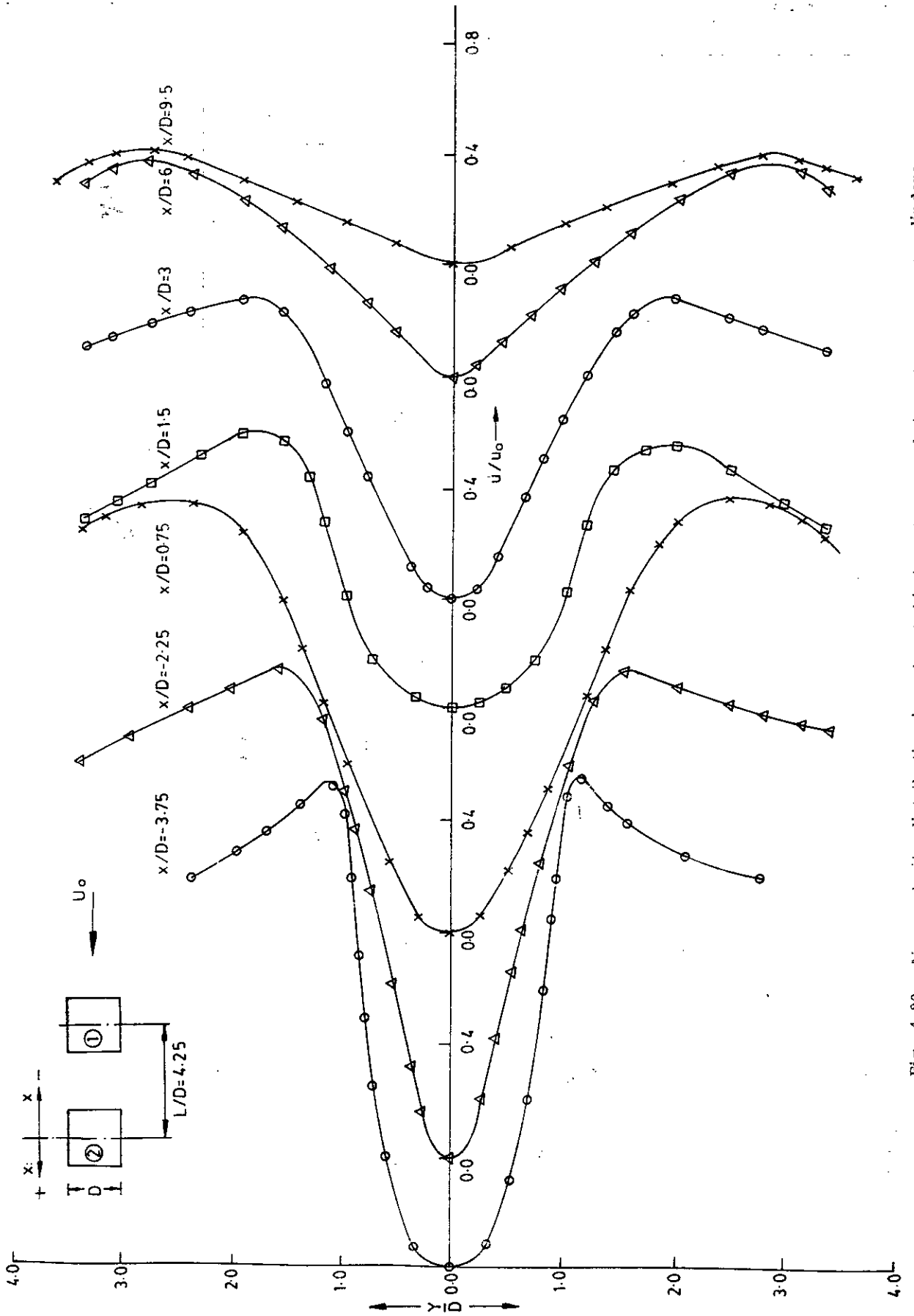


Fig. 4.20 : Mean velocity distribution in wakes behind upstream and downstream square cylinders arranged in tandem for $L/D = 4.25$

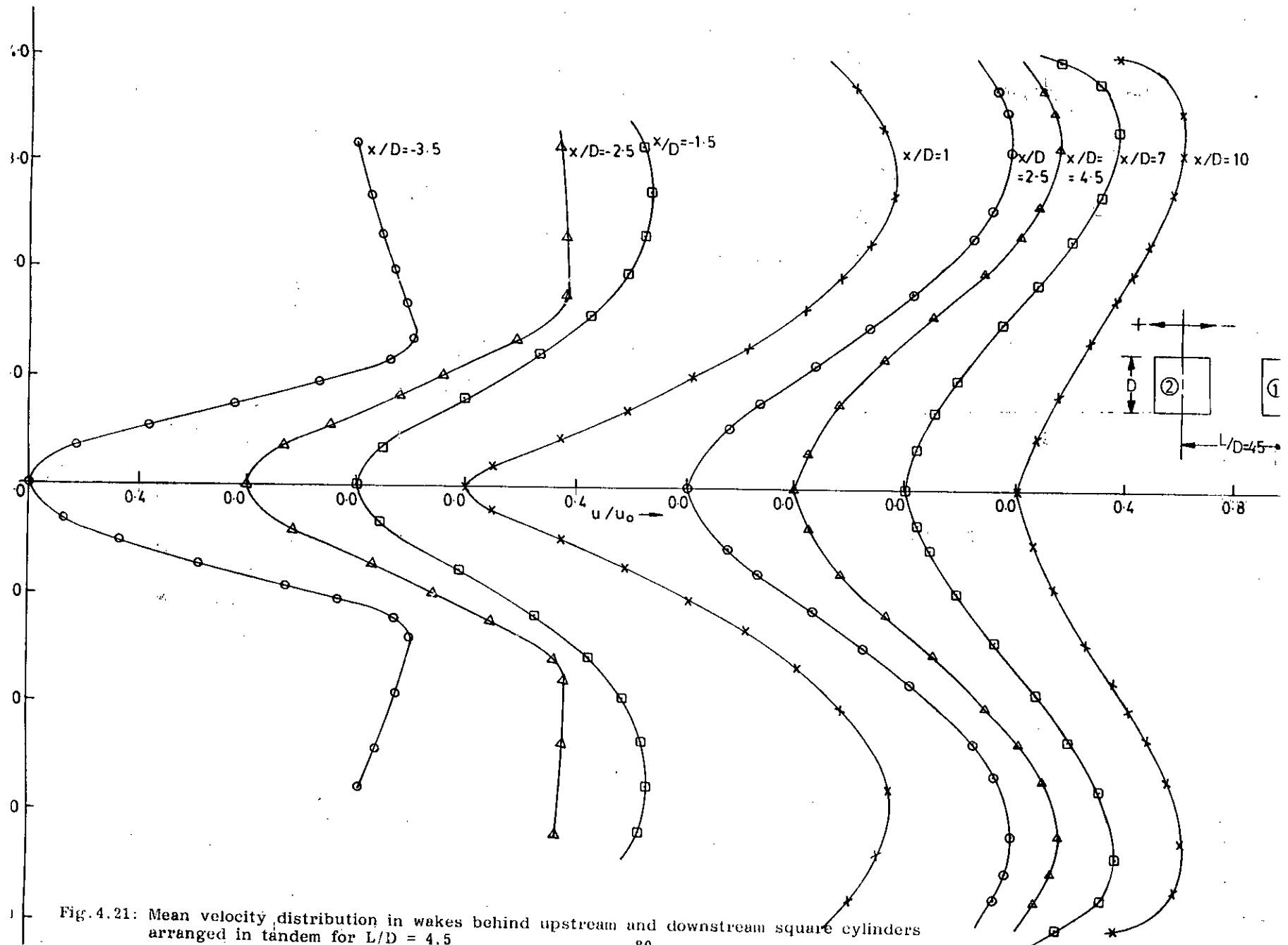


Fig. 4.21: Mean velocity distribution in wakes behind upstream and downstream square cylinders arranged in tandem for $L/D = 4.5$

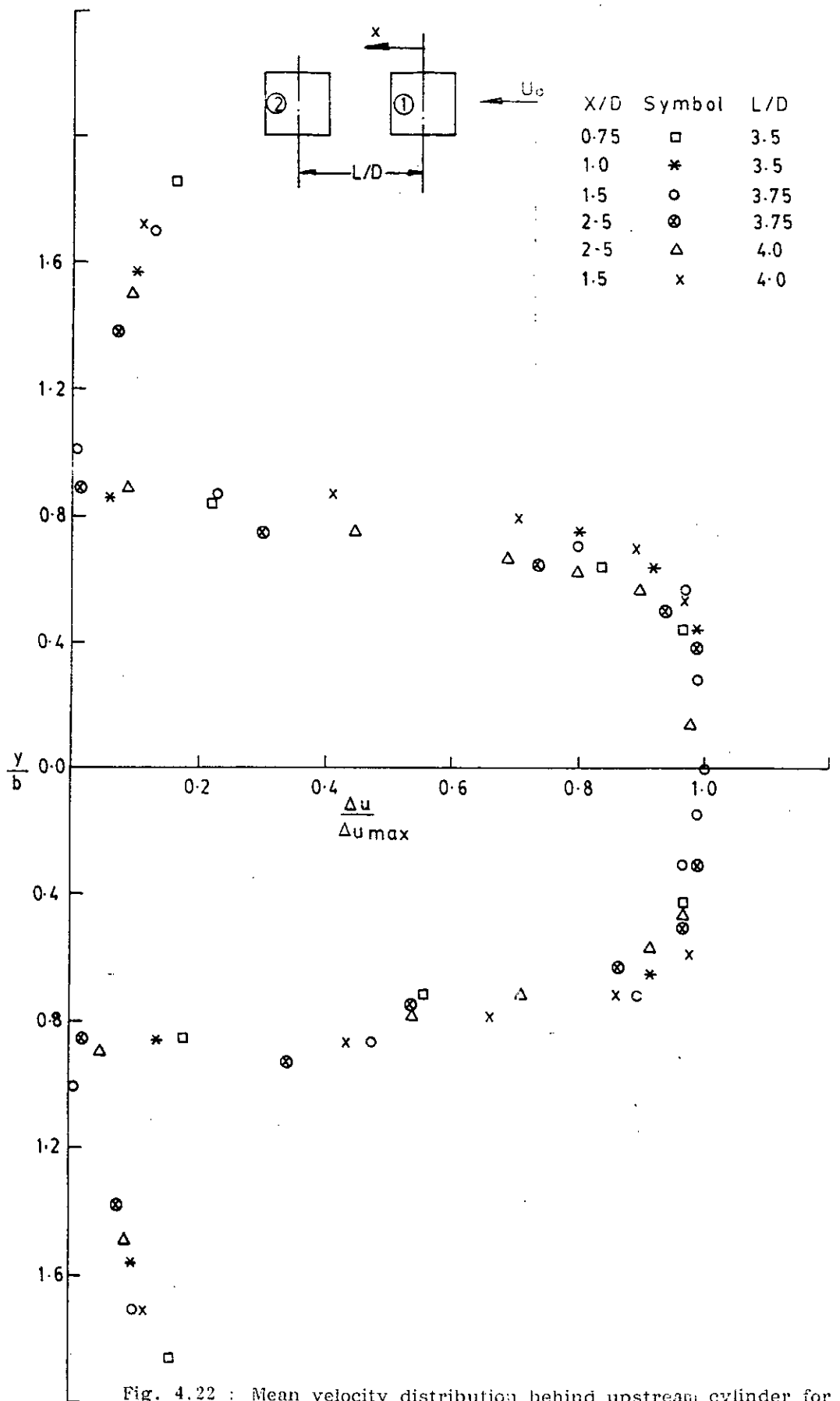


Fig. 4.22 : Mean velocity distribution behind upstream cylinder for longitudinal spacing $L/D = 3.5$ to 4.0 .

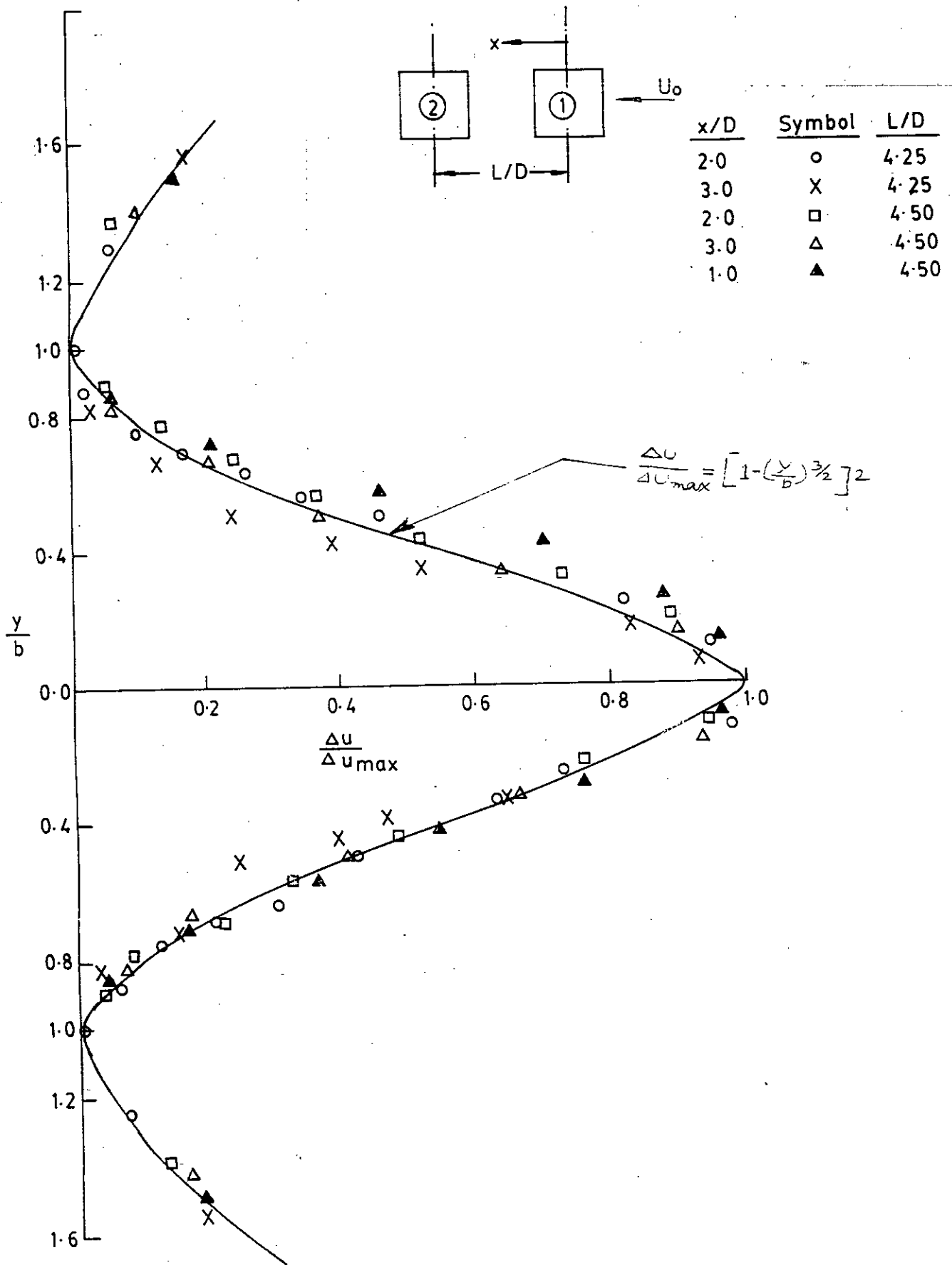


Fig. 4.23 : Mean velocity distribution behind upstream cylinder for longitudinal spacing $L/D > 4$.

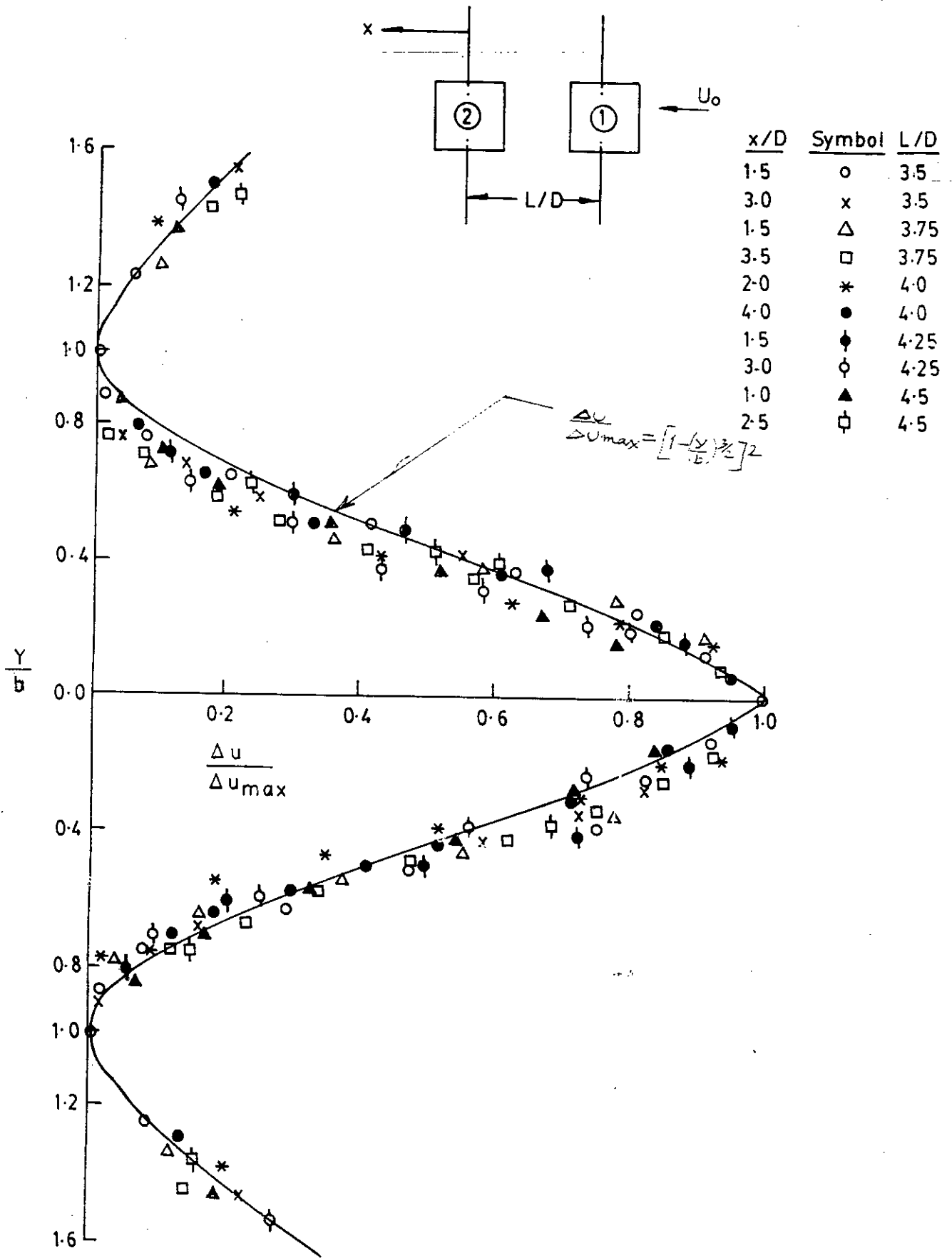
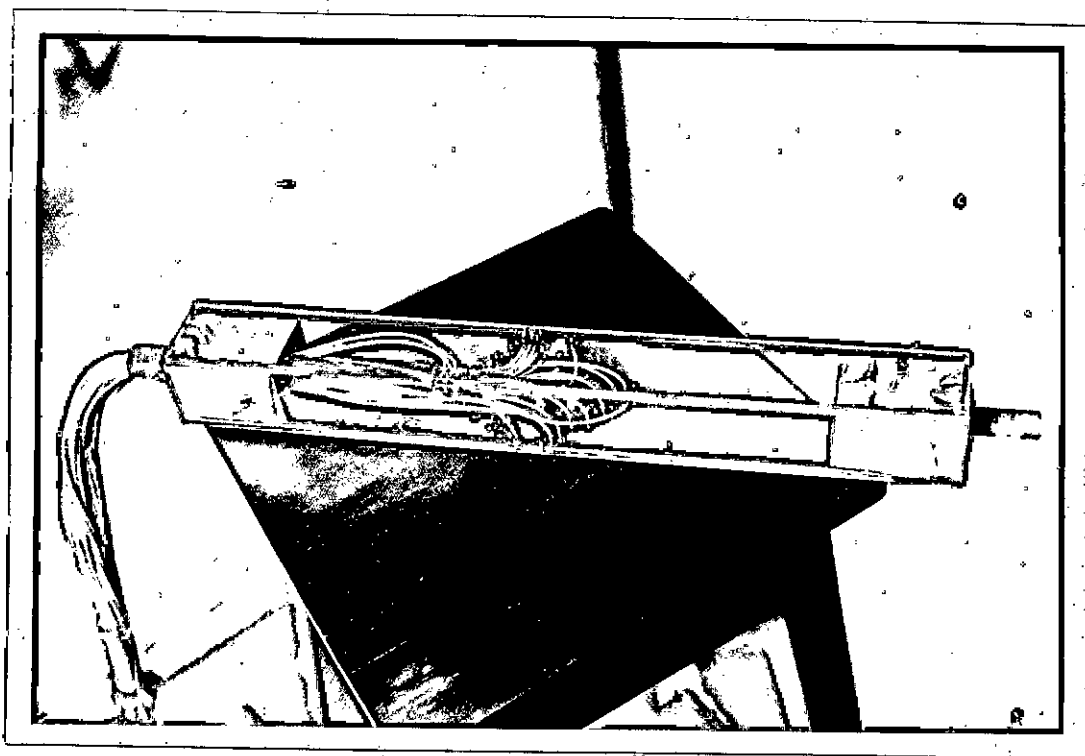


Fig. 4.24 : Mean velocity distribution behind downstream cylinder for longitudinal spacing $L/D = 3.5$ to 4.5 .

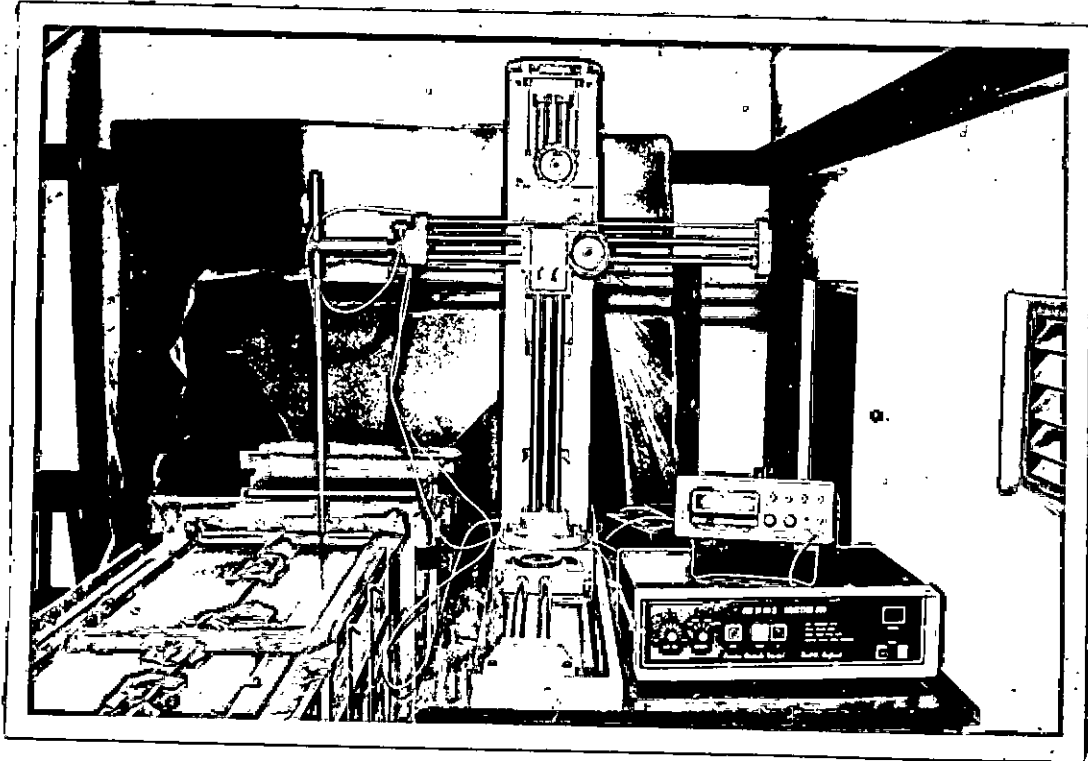
Table - 4.1

Authors	Cylinder size	Turbulent Intensity	Reynolds number	C_d
Present Measurement	50 mm x 50 mm	0.17%	6.05×10^4	2.33
A.C. Mandal (1975)	30 mm x 30 mm	0.4%	5.46×10^4	2.10
B.E. Lee (1975)	165 mm x 165 mm	4.4%	1.76×10^5	1.99
B.E. Lee (1975)	165 mm x 165 mm	12.5%	1.76×10^5	1.53
Pocha (1971)	165 mm x 165 mm	-	-	2.06

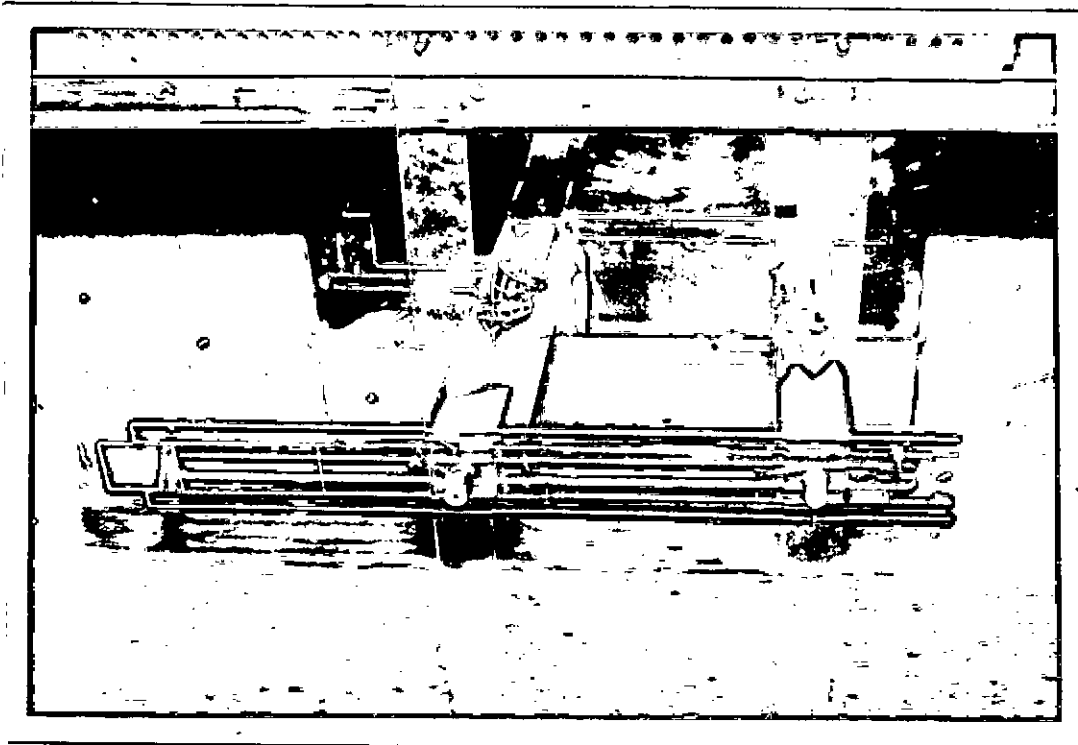
4.1 ; Variation of drag co-efficient of present and other cases at various Reynolds numbers with different turbulence intensity.



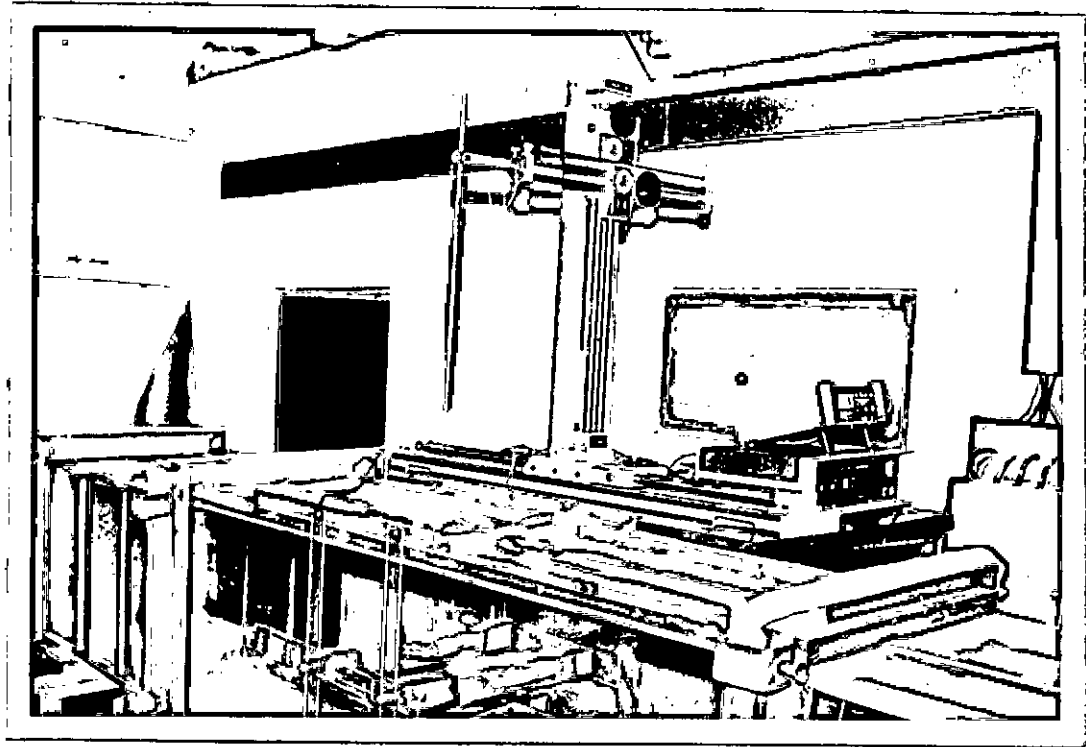
3.1 ; Square cylinder with tapplings.



3.2 : Co-ordinate measuring machine and pressure transducer.



3.3 : Square cylinders arranged in tandem in test section.



3.4 : Complete experimental set-up.

